International Journal of Biological Macromolecules 270 (2024) 132238

Contents lists available at ScienceDirect

International Journal of Biological Macromolecules

journal homepage: www.elsevier.com/locate/ijbiomac

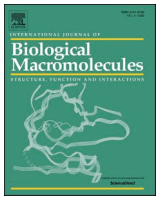

Review

Classification and functional origins of stereocomplementary alcohol dehydrogenases for asymmetric synthesis of chiral secondary alcohols: A review

Lu Zhang [1], Zewen Sun [1], Guochao Xu [*], Ye Ni [*]

Key Laboratory of Industrial Biotechnology, Ministry of Education, School of Biotechnology, Jiangnan University, Wuxi 214122, Jiangsu, China

ARTICLE INFO

Keywords:
Alcohol dehydrogenase
Stereocomplementary
Catalytic mechanism

ABSTRACT

Alcohol dehydrogenases (ADHs) mediated biocatalytic asymmetric reduction of ketones have been widely applied in the synthesis of optically active secondary alcohols with highly reactive hydroxyl groups ligated to the stereogenic carbon and divided into (*R*)- and (*S*)-configurations. Stereocomplementary ADHs could be applied in the synthesis of both enantiomers and are increasingly accepted as the "*first of choice*" in green chemistry due to the high atomic economy, low environmental factor, 100 % theoretical yield, and high environmentally friendliness. Due to the equal importance of complementary alcohols, development of stereocomplementary ADHs draws increasing attention. This review is committed to summarize recent advance in discovery of naturally evolved and tailor-made stereocomplementary ADHs, unveil the molecular mechanism of stereoselective catalysis in views of classification and functional basis, and provide guidance for further engineering the stereoselectivity of ADHs for the industrial biosynthesis of chiral secondary alcohol of industrial relevance.

1. Introduction

Biocatalytic asymmetric reduction, which utilizes enzymes or cells as biocatalysts instead of chemical catalysts, can achieve 100 % theoretical yield in reducing prochiral ketones into chiral secondary alcohols, which are important building blocks in the fields of agrochemicals, pharmaceuticals, food ingredients and materials, etc. [1]. Promoted by increasingly demands of agrochemicals and fine chemicals, biocatalysis and biosynthesis are generally accepted as the "*first-of-choice*" in organic synthesis [2–4]. Consequently, development of robust enzymes with superior adaptability to industrial conditions and efficient biosynthetic processes with high atomic economy and low environmental factor have drawn increasingly attentions.

Alcohol dehydrogenases (ADHs), also termed as carbonyl reductases (CR) or ketoreductases (KREDs), are commonly employed in the biocatalytic oxidation of alcohols and reduction of carbonyl compounds due to their high activity and stereoselectivity [5–8]. Being a redox reaction by nature, the oxidation or reduction reaction has to be accompanied by reduction or oxidation reaction of stoichiometric cosubstrates. ADHs utilize nicotinamide cofactors [ribose-phosphorylated (NADP) and ribose-nonphosphorylated (NAD)] for this. Since their role in host organism, ADHs exhibit high selectivity for cofactors. ADHs involved in anabolic pathways generally favor NADPH, while ADHs related to metabolism utilize NADH [9]. Therefore, in the practical application of ADH, the addition of expensive cofactors is indispensable.

Moreover, distinct from the hydrolases catalyzed enantioselective resolutions reactions, ADHs mediated bioreduction or biooxidation reactions are of special advantageous such as high atomic economy, in addition to mild reaction conditions, low environmental factor and high environmental beingness [9]. All these merits render ADHs promising for biomanufacturing. In addition, the catalytic performance of ADHs in the presence of organic solvents is often important since most prochiral ketones are highly hydrophobic. However, many ADHs exhibit decreased activity and stability in the presence of water-miscible organic solvents. As a result, a number of wild-type ADHs and their engineered variants with distinct enzyme properties such as enhanced activity, thermostability, stereoselectivity, substrate scope and organic solvent tolerance have been identified and developed, enriching the biocatalytic tool-box for the synthesis of chiral secondary alcohols [10]. For example, organic solvent tolerance of *Kp*ADH from *Kluyveromyces polyspora* was semi-rationally evolved and variants S237G and V231D with 3-fold improvement of organic solvent tolerance were obtained [11].

* Corresponding authors.
E-mail addresses: guochaoxu@jiangnan.edu.cn (G. Xu), yni@jiangnan.edu.cn (Y. Ni).
[1] Lu Zhang and Zewen Sun contributed equally to this work.

https://doi.org/10.1016/j.ijbiomac.2024.132238
Received 28 January 2024; Received in revised form 17 April 2024; Accepted 7 May 2024
Available online 9 May 2024

Although enzyme immobilization is widely used to improve stability of ADHs, the industrial application is still limited.

ADHs (EC 1.1.1.X, X = 1 or 2) belong to the oxidoreductase superfamily with unparalleled chemoselectivity, regioselectivity and stereoselectivity under benign conditions. In the past years, ADH-catalyzed asymmetric reduction reactions have been extensively studied and applied in the synthesis of chiral secondary alcohols. ADHs usually exhibit wide substrate spectrum toward ketones with diverse structures [12], such as methyl ketones, α-functionalized ketones, dicarbonyl compounds, γ- and δ-ketoesters, etc. ADHs could not only catalyze asymmetric reduction of ketones containing bulky-small substituents with high stereoselectivity, but also show activity toward "difficult-to-reduce" bulky-bulky ketones. A series of diaryl ketones could be reduced into the corresponding optically active diaryl alcohols with high yields and stereoselectivities using ADHs, which are often challenging in conventional chemical reactions [13,14]. According to the Cahn-Ingold-Prelog (Prelog) rule, asymmetric reduction of prochiral ketones by ADH follows Prelog or anti-Prelog priorities, depending on the direction of H transferring from NAPDH to the carbonyl C atom of substrate. Stereocomplementary ADHs refer to a pair of ADHs obeying opposite priorities in the asymmetric synthesis of (*R*)- or (*S*)-alcohols. Stereocomplementary ADHs are of great importance for preparing industrial relevant chiral alcohols and elucidating molecular mechanism of stereoselectivity control.

Considering the different but important effects of complementary chiral compounds, the stereoselective synthesis is of special interests not only in the research stage but also in application. To obtain a pair of chiral secondary alcohols, it is necessary to develop corresponding stereocomplementary ADHs. Screening of naturally evolved ADHs has been one of the main approaches for identifying ADHs with complementary stereoselectivity. Several pairs of ADHs have been reported, such as TR-I and TR-II, PseDH and EDH, etc. [6]. However, wild-type ADHs usually follow Prelog priority in the reduction of prochiral ketones, while ADHs obeying anti-Prelog rule are rare and usually have unsatisfactory properties with low activity and thermostability [15]. Hence, various strategies including random mutagenesis, semi-rational and rational engineering have been developed to construct ADHs with complementary stereoselectivities. Several tailor-made ADHs with high stereoselectivities have been successfully developed and applied in the synthesis of both enantiomers of secondary alcohols [13,16,17]. Great progress has been made in these fields. The application of ADHs in the synthesis of pharmaceuticals has been well reviewed [2]. However, the phylogenetic and functional basis of stereocomplementary ADHs has not been reported [15,18]. Consequently, this review is committed to highlight recent progress on the discovering and engineering of stereocomplementary ADHs and the functional basis for stereoselectivity control.

2. Classification and nomenclature of alcohol dehydrogenases

Alcohol dehydrogenases (ADHs), also known as carbonyl reductases (CRs) and ketoreductases (KRED)s, refer to a collective term of enzymes with activities in the reduction of ketones and oxidation of alcohols. ADHs are widely distributed in nature, including bacteria, fungi, plants, and animals, and play crucial roles in cellular metabolism and organic compound synthesis. Based on protein sequence and three-dimensional structure, ADHs can be divided into three families: short-chain dehydrogenase/reductase (SDR), medium-chain dehydrogenase/reductase (MDR), and aldo-keto reductase (AKR) [19].

Among ADHs, SDRs are named as the enzymes with the shortest chain length, usually of 250–350 residues. The activities of SDRs are not dependent on metal ions. However, Mg^{2+} could activate SDRs such as *Lb*ADH and *Sc*CR through stabilizing the stereostructure of SDRs. So far, over 160,000 SDRs sequences have been recorded in GenBank, with 53,037 crystal structures available in the Protein Data Bank (PDB). Based on the conserved sequence motifs of SDRs proposed by Kallberg et al., ADHs can be divided into seven subclasses: Classical, Extended, Atypical, Intermediate, Divergent, Complex, and Unassigned SDRs [17,20,21].

Although the similarity in amino acid sequence of different SDRs subfamilies is merely 20–30 %, most SDRs share similar three-dimensional structures, including a Rossmann fold domain for binding of NAD(*P*)H and a loop-rich region forming the active center. Taken methylglyoxal/isovaleryl aldehyde reductase Gre2 from *Saccharomyces cerevisiae* (PDB ID: 4PVD) as example (Fig. 1A) [22], it is a typical Extended SDR with 341 residues with N-terminal for cofactor binding and C-terminal for substrate binding. The cofactor binding domain has a typical Rossmann structure composed of parallel seven *β*-folds and *α*-helices, which are commonly found in all SDRs [23]. About the 20th residue downstream of the conserved sequence GXXXGXG at *N*-terminal determines the cofactor (NADH/NADPH) preference of SDRs. Acidic residues at this position can specifically bind to the 2′ and 3′ hydroxyl groups on the NAD(H) ribose ring, while basic residues play an important role in binding with NADP(H) through electrostatic interaction between phosphor group of NADP(H) and basic side chain [24]. The highly conserved catalytic triad, Ser-Tyr-Lys, locates in the middle of the amino acid sequence. C-terminal sequences of SDRs are less consensus, indicating diverse substrate specificity of different SDRs. In the catalytic triad, Tyr acts as the core catalytic residue, while Ser exhibits a stabilizing effect on the carbonyl of substrate, and Lys forms a hydrogen bond with the hydrogen of nicotinamide ring to facilitate proton transfer. Reaction starts with a proton transfer from Tyr-OH to the carbonyl O atom of the substrate, followed by a H transfer from the coenzyme NAD(*P*)H to the carbonyl C atom of the substrate, resulting in the reduction of the carbonyl to an alcohol (Fig. 1A) [25]. Another type of catalytic residue of SDRs is tetrad including Asn-Ser-Tyr-Lys. The carbonyl group of Asn forms a characteristic helical kink structure by forming hydrogen bond interactions with Lys and water molecules surrounding Lys, which could significantly activate the catalytic function of Lys [25,26].

Medium-chain dehydrogenases (MDRs) have an amino acid length longer than SDRs, typically around 350 residues. MDRs can be directly divided into 86 different subfamilies, such as MDRO01-ADH and

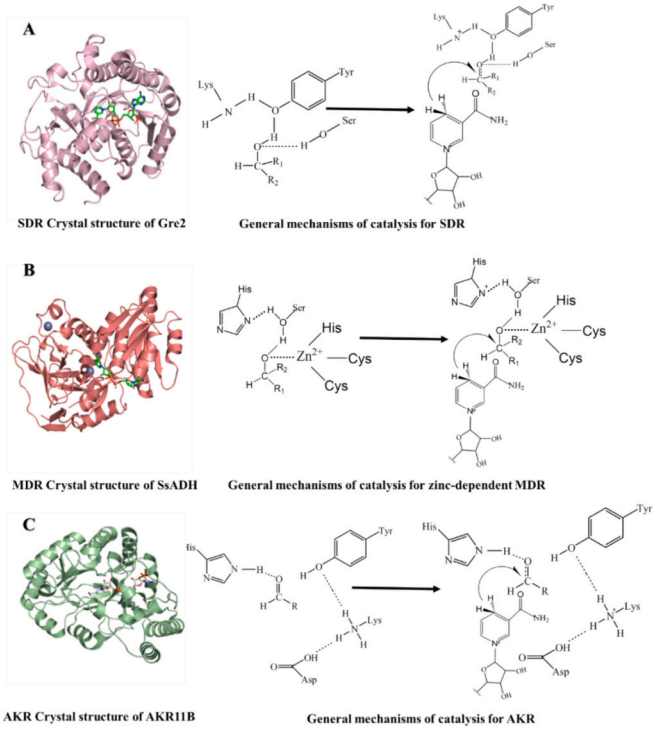

Fig. 1. Crystal structures and general catalytic mechanisms of various ADHs.

MDRO03-FAS, etc. Sequence similarity of different subfamilies of MDRs is higher than that of SDRs, reaching 40–90 %. Similar to SDRs, MDRs are generally monomers, dimers, and tetramers, such as *Ss*ADH from *Saccharolobus solfataricus* (PDB ID: 1R37) (Fig. 1B). One subunit of MDRs typically consists of two parts. One cleft structure responsible for substrate binding is formed by folding of N- and C-terminal residues, the other is Rossmann fold for cofactor binding, similar to that of SDRs. Most of MDRs from eukaryotes typically require the assistance of Zn^{2+} to exert their catalytic functions. Zn^{2+} often plays a catalytic role by forming a tetrahedral structure containing carboxyl ligands with conserved residues Cys-His-Lys (Fig. 1B). The carbonyl substrate initially enters the active site and interacts with the tetrahedral structure and two hydroxyl groups on the ribose ring of the cofactor. Subsequently, H from C4 of the reduced cofactor is received by catalytic conformation of substrate, resulting in the conversion of ketone to its corresponding alcohol product [27–29]. MDRs from prokaryotes are non-Zn^{2+}-dependent enzymes and only display reductive activity. On the contrary, Zn^{2+}-dependent MDRs from eukaryotes show both oxidative and reductive activities [30–31]. The structural and functional differences among MDRs from different sources could explain their differences in catalytic activities.

Aldo-keto reductases (AKRs) typically possess around 320 amino acids and belong to non-metal-dependent dehydrogenases. AKRs are widely distributed in mammalian, plant, and microbial cells. AKRs superfamily contains >190 members that can be divided into 16 subfamilies, designated as AKR1 to AKR16 [19]. Unlike SDRs and MDRs, most of AKRs exist as monomers. Although their catalytic activities are consistent with SDRs and MDRs, three-dimensional structures of AKRs are quite different [32]. Take AKR11B from *Bacillus subtilis* (PDB ID: 1PZ1) as an example (Fig. 1C) [33], the Rossman fold structure for cofactor binding does not exist in AKR11B. The overall structure has a conserved $(\alpha/\beta)_8$-barrel TIM structure, specifically, a barrel-shaped structure composed of eight β-folds arranged in a twisted manner, surrounded by eight α-helices. Catalysis of ADRs is promoted by a conserved tetrad of active site residues including Asp-Tyr-Lys-His. Substrate specificity of AKRs is determined by three loops, and the cofactor binds to the central region of the TIM structure [34,35]. The phenolic hydroxyl group of Tyr provides general acid-catalytic assistance for carbonyl reduction through enzyme-bound NAD(*P*)H, followed by H transfer from coenzyme NAD(*P*)H to carbonyl C atom, leading to reduction of carbonyl group to hydroxyl group (Fig. 1C) [36]. AKRs have a broader substrate spectrum than SDRs and MDRs, and can catalyze the reduction of various substrates such as acetone, aldose sugars, aldoses, aldehydes, and acetaldehydes [37,38].

Although ADHs of SDRs, MDRs and AKRs are distinct in stereostructure and catalytic residues, all of them are important biocatalysts in the asymmetric preparation of chiral secondary alcohols employing different mechanisms. Their crystal structures provide interesting evidences for unveiling the origin of stereoselectivity control.

3. Prelog and anti-Prelog rule of alcohol dehydrogenases

ADHs follow the sequential Bi—Bi kinetic mechanism to catalyze the asymmetric reduction of prochiral ketones. ADH binds with cofactor NAD(*P*)H to form a holoenzyme, followed by the entering of ketone substrates into the active center to form an ADH-substrate complex. The substrate obtains one H from catalytic Tyr and another H transferred from the reducing cofactor, and the ketone is reduced into the corresponding chiral alcohol. At the same time, NAD(*P*)H is oxidized into $NAD(P)^+$. Finally, the chiral alcohol and $NAD(P)^+$ are released from the active center. In the asymmetric reduction, ADHs exert its catalytic function in the presence of NAD(*P*)H, which acts not only as hydrogen donor but also forms hydrogen bond with catalytic residues of ADHs [39].

The Cahn-Ingold-Prelog (Prelog) rule has become an integral part of chemical nomenclature since 1956, providing a convenient way to identify the relative stereostructure of a chiral center. According to Prelog rule, the chirality of the stereogenic center is defined as *pro-R* or *pro-S* based on the priority order of groups attached to the chiral center [40]. As shown in Fig. 2, prochiral carbon atom of ketone substrates is a sp^2-hybridized carbon, forming a planar structure with large (R_L) and small (R_S) substituents on both sides of the carbonyl group. According to the Prelog rule, two planar sides are designated as *re*-face and *si*-face. When hydride of cofactor nucleophilically attacks the carbonyl carbon of the substrate, the relative position of hydrogen anion to the substrate plane determines stereoselectivity of ADHs. When the H attacks from the *re*-face of the plane, the reaction follows the Prelog rule and generates (*S*)-alcohol (*pro-S* attack). Conversely, when the H attacks from the *si*-face, the reaction follows the *anti*-Prelog rule and generates (*R*)-alcohol (*pro-R* attack) [41].

As early as 1986, Keinan et al. studied the alcohol dehydrogenase *Tb*ADH from *Thermoanaerobacter brockii* and proposed the "large pocket" and "small pocket" theory for discriminating different substrate binding modes based on the enzyme-substrate complex structure. It was proposed that the substrate is stabilized into the active center of enzyme when the size and orientation of two substituents of carbonyl group are complementary to the shape, electrostatic, hydrophobicity of the enzyme's active center. Molecular docking and molecular dynamics (MD) simulations were conducted on the modification of short-chain alcohol dehydrogenase *Eb*SDR8 from *Empedobacter brevis* ZJUY-1401, and the introduction of Y188G could increase the size of the substrate binding pocket, leading to increased stereoselectivity (99 % *S*) toward aryl ketone esters [42]. Qin et al. switched the stereoselectivity of *Cg*KR1 from *Candida glabrata* for asymmetric reduction of 2-chloroacetophenone and 2-chloro-4′-fluoroacetophenone between Prelog and *anti*-Prelog by modulating substrate binding pocket size [43].

Except for the spatial steric effect, electrostatic and hydrophobic interactions between enzyme and substrate also have profound impacts on stereoselectivity. When the difference between both sides of substrate substituents is limited, the spatial steric effect on stereoselectivity is compromised, and interactions between substrate and ADH become the major factors in manipulating stereoselectivity. For example, (i) "Polar Gate" structure of *Kp*ADH at the entrance of the active site pocket [44]; (ii) aromatic stacking interactions formed between enzyme and substrate [45]; (iii) hydrophobic/hydrophilic of substrate binding pocket residues [39,46].

Enzyme stereoselectivity is also influenced by reaction conditions such as temperature, pH, and reaction medium. Phillips et al. found that secondary alcohol dehydrogenase from *Thermoanaerobacter ethanolicus* (SADH) shows reversed stereoselective preference with increasing temperature [18]. At temperatures below 26 °C, SADH preferentially catalyzed production of (*S*)-butanol, while at above 26 °C, stereoselective preference of SADH switches to (*R*)-butanol. Changes in entropy and enthalpy with temperature promote the exclusion of water molecules from the enzyme active site, thereby favoring the formation of the (*R*)-enantiomer at higher temperatures [39]. Li et al. reported that the addition of different cosolvents can affect the stereoselectivity of *Ss*CR in reduction of (4-chlorophenyl)(pyridine-2-yl) ketone (CPMK). When 10 % tetrahydrofuran is added, the stereoselectivity was increases from 50 % to 88 % [47]. Using *Saccharomyces cerevisiae* type II as catalyst, 2-octanone as substrate, and water/n-dodecane biphasic system as the reaction system, the effect of organic solvent on expression of ADH 1–3 isoenzymes and asymmetric reduction of 2-octanone were evaluated. The results indicate that the suppressed expression of ADH-2 could potentially improve the stereoselectivity of asymmetric reduction, while overexpression of ADH-2 may reduce the stereoselectivity [48].

4. Naturally evolved stereocomplementary alcohol dehydrogenases

Natural evolution tends to retain enzymes with the highest adaptability. More ADHs obeying Prelog priority are identified than ADHs

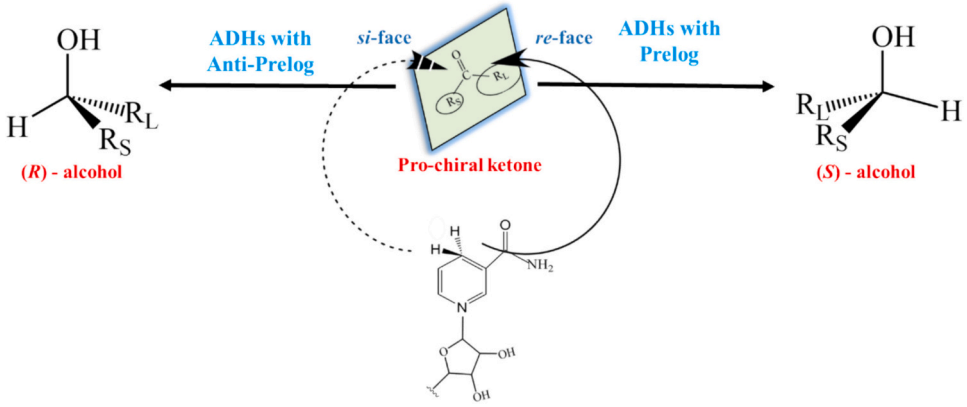

Fig. 2. Stereoselectivity origin of Prelog and anti-Prelog ADHs.

following anti-Prelog priority. Only few stereocomplementary ketoreductases have been reported. Based on specific genome libraries and online databases, screening of natural enzymes with opposite stereoselectivity toward a particular substrate has become one common method to identify stereocomplementary enzymes. In recent years, many researchers have screened specific ADH libraries to obtain highly stereoselective natural stereocomplementary ADHs for the synthesis of corresponding enantiomers. The development of stereocomplementary

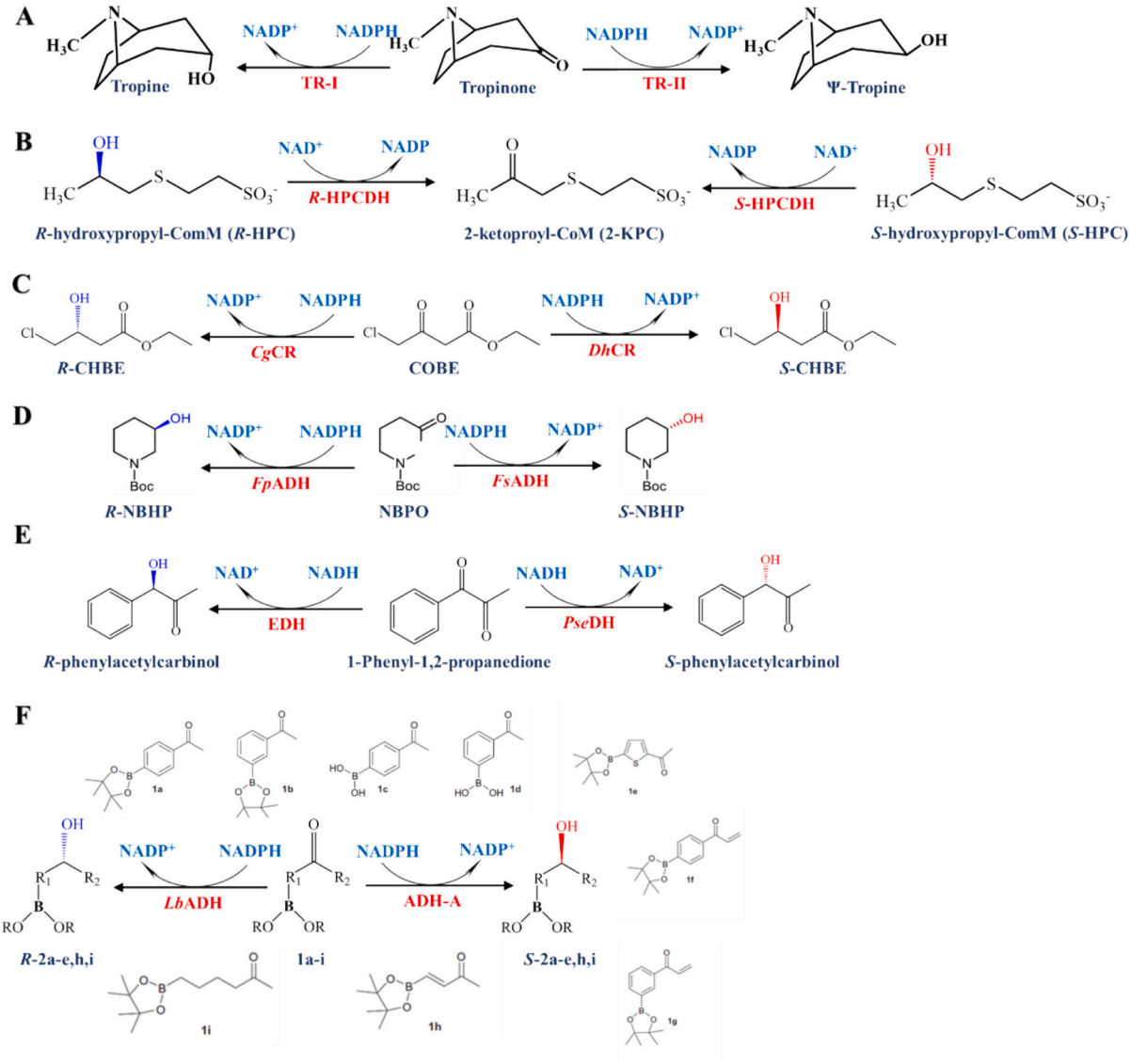

Fig. 3. Asymmetric preparation of chiral hydroxyl compounds by stereocomplementary ADHs. **(A)** TR-I and TR-II, **(B)** *R*-HPCDH and *S*-HPCDH, **(C)** *Cg*CR and *Dh*CR, **(D)** *Fp*ADH and *Fs*ADH, **(E)** EDH and *Pse*DH, **(F)** *Lb*ADH and ADH-A.

ADHs can not only contribute to a deeper understanding of molecular mechanisms of stereoselectivity control, but also provide guidance for tailor-made engineering the stereoselectivity of ADHs.

4.1. TR-I and TR-II from Datura stramonium

Tropinone is an important intermediate for tropane alkaloid biosynthesis, which can be reduced to tropine or pseudotropine (ψ-tropine) by NADPH-dependent tropinone reductase I (TR-I) and II (TR-II) from *Datura stramonium*. Sequences of TR-I and TR-II indicate that both of enzymes belong to SDR family. These two TRs are considered to be homodimers sharing sequence identity of 64 % in amino acids sequence, and have strict stereoselectivity in the reduction of tropinone. TR-I catalyzes the reduction of tropinone into tropine with 3α-hydroxyl group, while TR-II catalyzes the reduction of tropinone to ψ-tropine with 3β-hydroxyl group (Fig. 3A) [49,50]. TR-I and TR-II have different K_m values toward tropinone, however, similar K_m values toward NADPH. These results show that the different stereospecificities of two TRs are determined by the binding mode of tropinone instead of NADPH. A comparison of crystal structures of TR-II-NADPH and TR-II-NADPH-tropinone complexes revealed that substrates tropinone undergoes a rotational movement, which is complementary to the spatial organization of the active site and favorable for the proceeding of reaction, and results in stereospecific differences between TR-I and TR-II. The substitution of five residues (L210, E156, S148, Y159 and K163) in TR-II enzyme led to a nearly complete reversal of stereospecificity, indicating the binding orientation of tropinone determines the stereospecificities. Kinetic analysis of TR variants reveals that the contributions of electrostatic and hydrophobic interactions are crucial in determining the stereospecificity of TR. The discovery of TR1 and TRII demonstrates that different charged residues around the substrate binding site are critical in stereoselectivity control [51–53].

4.2. R-HPCDH and S-HPCDH

The (*R*)- and (*S*)-enantiomers of 2-hydroxypropylthio ethanesulfonate (HPC) are oxidized into achiral product 2-oxopropyl-CoM by (*R*)-hydroxypropyl coenzyme M dehydrogenase (*R*-HPCDH) and (*S*)-hydroxypropyl coenzyme M dehydrogenase (*S*-HPCDH), which share 41 % identity in amino acid sequence (Fig. 3B). The *R*- and *S*-HPCDH are homologous enzymes and both belong to SDR family [54,55]. By comparing the crystal structures of *R*-HPCDH and *S*-HPCDH, and effects of linear alkylsulfonates on kinetics and stereoselectivity, electrostatic interactions between the O atom of sulfonic acid and the Arg residue were found to be crucial in determining the reactive conformation of substrates for chiral discrimination. This strong ionic interaction facilitates the proper orientation of the hydroxy group and hydrogen atom of the alcohol. The catalytic triad of *S*-HPCDH is composed of Y156-K160-S143, while R211 and K214 are identified as the residues that interact with the sulfonic acid group of CoM in *S*-HPC. However, *S*-HPCDH3 cannot bind *R*-HPC in the same way, likely due to spatial conflicts imposed by the orientation of CoM- and methyl binding pockets (Fig. 4A). Different strategies controlling stereoselectivity of *R*- and *S*-HPCDH reveal that the substrate and cofactor binding pockets affect the orientation of the substrate through coordination bonds, thereby controlling the stereoselective preferences of ADHs [56,57].

4.3. DhCR and CgCR

A pair of stereocomplementary carbonyl reductases, *Dh*CR and *Cg*CR, were identified from *Debaryomyces hansenii* and *Candida glabrata* with high activity and stereoselectivity for asymmetric reduction of aromatic *β*-ketonitriles (Fig. 3C). In a biphasic system, use of *Dh*CR and *Cg*CR has completely eliminated competition of α-ethylation in biocatalytic reduction of aromatic *β*-ketonitriles. Employing recombinant *Escherichia coli* whole cells coexpressing stereocomplementary carbonyl reductases and glucose dehydrogenase from *Bacillus megaterium* (*Bm*GDH) was advantageous for the application in scale-up synthesis of chiral *β*-hydroxy nitrile with >99 % *ee* and 92 % yield at substrate loading of 145 g/L. (*S*)- and (*R*)-CHBE were synthesized by *Dh*CR and *Cg*CR with around 93.0 % yields and >99 % *ee* at 330 g/L COBE. In addition, *Dh*CR and *Cg*CR were able to catalyze the asymmetric reduction of 7 chiral haloalkanes with pharmaceutical relevance. The versatile performance of *Dh*CR and *Cg*CR demonstrates the enormous potential of stereocomplementary enzymes in industrial applications [58,59].

4.4. CgKR1 and CgADH

*Cg*KR1 and *Cg*ADH are enzymes derived from *Candida glabrata*, with 78 % sequence similarity, and their catalytic activities are expected to be highly similar [60]. Both *Cg*KR1 and *Cg*ADH are classified into SDRs superfamily. However, two enzymes display completely opposite stereoselectivity toward NBPO. *Cg*KR1 produced (*S*)-NBHP with *ee* value of 99 %., while *Cg*ADH produced (*R*)-NBHP in >99 % *ee* [61]. Both of enantiomers are important chiral building blocks for the synthesis of pharmaceuticals. Similar phenomenon was also found in the reduction of prochiral ethyl 4-chloro-3-oxobutanate (COBE). *Cg*KR1 produced (*S*)-ethyl 4-chloro-3-hydroxybutanate (CHBE) with 98 % *ee*, while *Cg*ADH produced (*R*)-CHBE in 99 % with *ee* Considering their high similarity in protein sequence and three-dimensional structure, the two naturally evolved stereocomplementary *Cg*KR1 and *Cg*ADH are interesting objects to understand the molecular basis of stereoselectivity control of ADHs.

4.5. FpADH and FsADH

Alcohol dehydrogenases from *Flavobacterium psychrophilum* (*Fp*ADH) and *Flavobacterium* sp. (*Fs*ADH), were identified as a pair of stereocomplementary ADHs, and exhibited high catalytic efficiency toward 3-

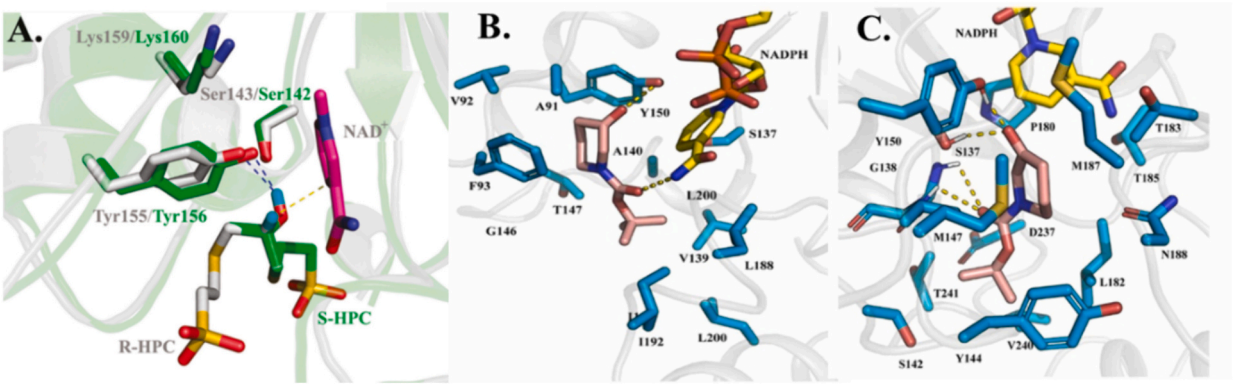

Fig. 4. Substrate-ligand interaction analysis of **(A)** *R*-HPCDH1 (gray) and *S*-HPCDH3 (green), **(B)** *Fp*ADH, **(C)** *Fs*ADH.

N-substituted-azacyclic (NBPO) substrates and broad substrate scope (Fig. 3D). For the asymmetric synthesis of (*S*)-NBHP, *Fs*ADH exhibited high stereoselectivity (>99 % *ee*) and space-time yield of 643.8 g/L/d, while *Fp*ADH produced (*R*)-NBHP with >99 % *ee* and STY of 497.3 g/L/d. Through molecular docking and MD simulations, the stability differences of the pre-reaction conformations between (*R*)-NBHP and (*S*)-NBHP in the active center of *Fp*ADH (Fig. 4B) and *Fs*ADH (Fig. 4C) result in the opposite stereoselectivity of two enzymes. The hydrogen bonding formed by Y150 and S137 at the catalytic site and the substrate side chains are responsible for the high catalytic efficiency of both enzymes. Except for NBPO, these two stereocomplementary enzymes also displayed opposite stereoselectivity toward other prochiral ketones including ketoesters, acrylates, and heterocyclic ketones [62].

4.6. *Pse*DH and EDH

Anti-Prelog stereospecific *Pse*DH and Prelog-specific EDH were both identified from *Arthrobacter* sp. TS-15 with full conversion and >99 % *ee* in regio- and enantio-specific reduction of 1-phenyl-1,2-propanedione into (*S*)-phenylacetylcarbinol and (*R*)-phenylacetylcarbinol (Fig. 3E). NAD(H)-dependent *Pse*DH and EDH are highly potential for industrial production of valuable chiral compounds, which catalyze the reduction of a wide range of substrates including arylaliphatic haloketones, diketones, ketoesters, aryl-aryl ketones, and bulky-bulky α-diketones. Amino acid sequence alignment demonstrates that *Pse*DH shares 32 % similarity with EDH. Crystal structural of *Pse*DH (6QHE) indicates that S143 and conservative residue D149 may be the key residues in determining the *anti*-prelog stereospcificity of *Pse*DH [63].

4.7. *Lb*ADH and ADH-A

Alcohol dehydrogenases from *Lactobacillus brevis* (*Lb*ADH) and *Rhodococcus ruber* DSM 44541 (ADH-A) could catalyze the reduction of boron-containing carbonyl compounds to corresponding (*S*)- and (*R*)-alcohols with high conversion ratios and >99 %, *ee* (Fig. 3F) [64]. ADH-A belongs to MDR superfamily with a monomer molecular weight of 38 kDa, and contains one Zn^{2+} per monomer. While *Lb*ADH belongs to NADP-dependent SDR superfamily that exhibits catalytic activity in dependence of Mg^{2+}. Despite their similar 3D-structures, minor differences in the active center are crucial for their opposite stereoselectivity.

5. Stereocomplementary alcohol dehydrogenases developed by protein engineering

Development of directed evolution, structure- and computation-guided enzyme engineering has broadened the application scope of biocatalysts. Based on different library construction approaches, enzyme engineering can be divided into three strategies: random mutagenesis, semi-rational engineering, and rational engineering [65]. Subsequently, libraries of variants are subjected to characterization such as stability, selectivity, and catalytic efficiency to discover tailor-made enzymes with enhanced functionality. Mutagenesis libraries with high quality and sensitive high-throughput screening methods are critical for the success of enzyme engineering [66]. Unlike screening for variants with high stability and activity, stereoselectivity relies on determination of *ee* values employing HPLC or GC equipped with chiral columns, which are often time-consuming. As a result, two approaches are important for efficient identification of tailor-made stereoselective variants: 1) development of '*small but smart*' libraries employing structural and computational guided strategies, 2) construction of high throughput screening strategies for determination of stereoselectivity.

Among naturally evolved enzymes, it is often difficult to obtain highly stereoselective stereocomplementary enzymes through gene mining. During the evolutionary process, the stereo-selectivity of enzymes may have evolved to achieve the optimal reactivity with substrates of a specific stereo-configuration to adapt to the specific physiological environment in organisms [15]. Additionally, the sequence similarity of naturally evolved stereocomplementary enzymes is generally low (e.g., the sequence similarity between stereocomplementary *Fp*ADH and *Fs*ADH is only 58 %), resulting in significant differences in their active pockets. More and more strategies have been developed to obtain stereocomplementary enzymes for the synthesis of enantiomers of secondary alcohols. More importantly, elucidating molecular mechanisms underlying the stereoselectivity control could provide useful guidance for engineering and de novo designing of stereocomplementary enzymes.

5.1. *Structure alignment-guided engineering of stereoselectivity with Prelog or anti-Prelog preference*

Stereoselectivity reversion was achieved by Yu et al. based on comparison of structures of *anti*-Prelog EbSDR8 from *Empedobacter brevis* ZJUY-1401 and *Pp*YSDR from *Pseudomonas putida* ATCC 12633 with Prelog stereopreference. Five single variants including M85T, M85V, M85S, W182V and L136V were capable of catalyzing the reduction of 2,2,2-trifluoroacetophenone to (*S*)-2,2,2-trifluoro-1-phenylethanol with 14–45 % *ee*, while the parent enzyme produced (*R*)-enantiomer with 57 % *ee*. The stereoselectivity of double variant M85T/W182V was completely inverted to 99 % (*S*) from 57 (*R*). Enzyme-substrate docking analysis showed that the increased spatial flexibility was achieved by replacing larger residues with smaller ones, which allows H attack from the *si*-face of the carbonyl group (**pro**-R attack) and leads to formation of *anti*-Prelog products (Fig. 5A). In addition, hydrogen bondings between mutated residues and halogen atom of substrate further stabilizes the *anti*-Prelog preferred conformation [67].

Six naturally occurring enzymes obeying Prelog or *anti*-Prelog rules were discovered to understand the switch between Prelog and *anti*-Prelog reduction toward halogen-substituted acetophenones. Based on structural information, multiple sequence alignment, and MD simulation were performed using *Lf*SDR1 (from *Lactobacillus fermentum*) as the starting enzyme. Three key residues including G92, E141 and V186 were identified as the potential sites governing stereoselectivity of *Lf*SDR1. Then, a pair of stereocomplementary variants *anti*-Prelog V186F and Prelog G92E/E141L/V186A were constructed for producing (*S*)- and (*R*)-2-chlorophenylethanol with >99 % *ee*. The interesting mutations identified in *Lf*SDR1 were also introduced in the counterpart positions of five homologous SDRs, and the stereoselectivities of these five homologous SDRs were also reversed from Prelog to *anti*-Prelog [43]. Small residues at 186 and medium to bulky residues at position 92 around substrate binding pocket are conducive to *pro-S* attack and generate Prelog enzymes. On the other hand, variants with bulky residues at position186 and small residues at position 92 are favorable for *pro-R* attack, and follow anti-Prelog rule (Fig. 5B).

5.2. *Inverted stereoselectivity of ADHs by structure-guided design of substrate-binding pocket*

For ADH with known crystal structures, substrate binding pocket analysis is an effective strategy to obtain variants with reversed stereoselectivity. Through altering the shapes and sizes of the binding pockets, the interaction network between the enzymes and substrates can be affected, thereby altered stereoselectivity.

NADH-dependent (*R*)-specific carbonyl reductase (RCR) belonging to MDRs was identified from *Candida parapsilosis*. RCR can catalyze asymmetric reduction of prochiral aryl ketones into corresponding alcohols with excellent *S*-stereoselectivity. It was found that F285 and W286 larger side chains locate at the entrance (F285) and inside (W286) of the small pocket. It was hypothesized that substitutions with Ala at these positions may alter conformation of substrate binding and influence the stereoselectivity. Variants W286A, F285A and F285A/W286A were obtained with completely inverted stereoselectivity toward 2-bromo-1-(4-chlorocyclohexyl)ethan-1-one and producing (*S*)-alcohol

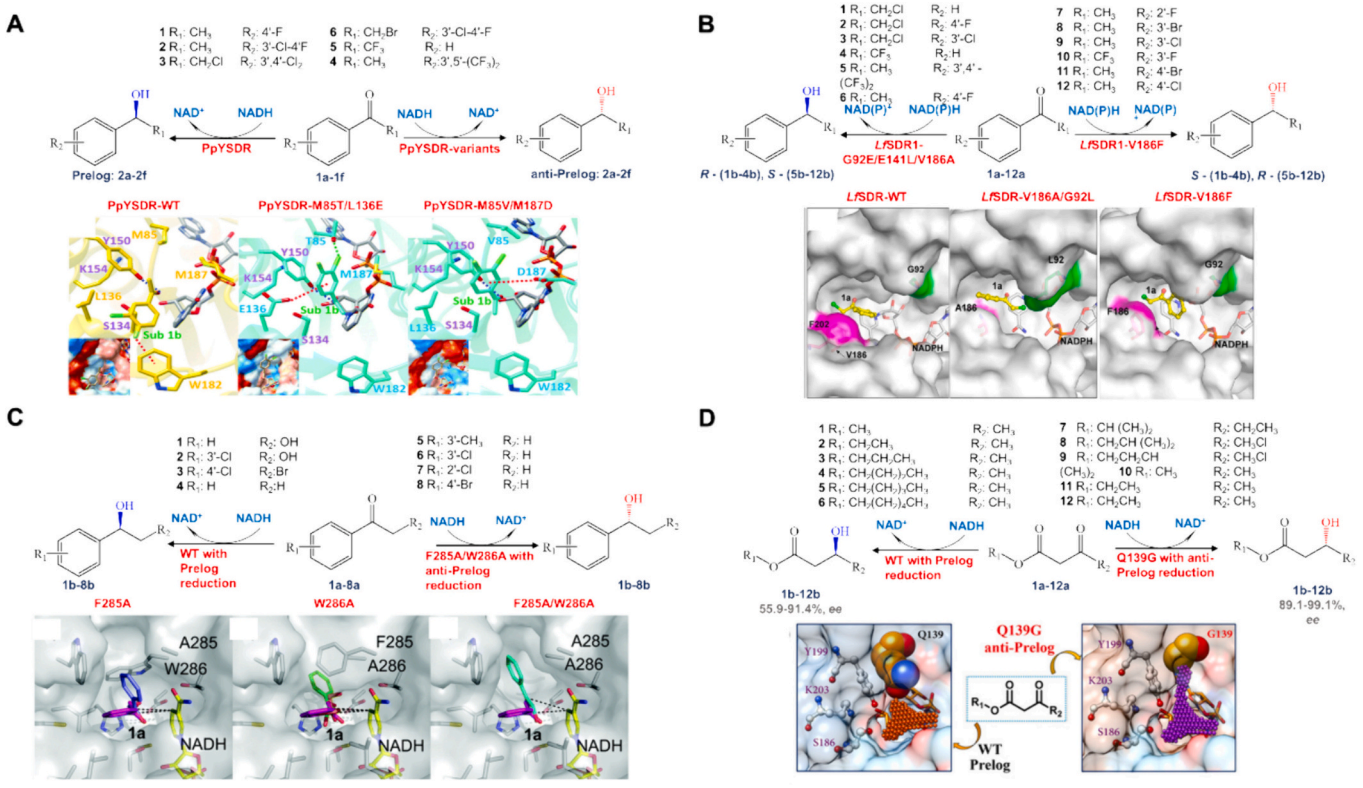

Fig. 5. Asymmetric reduction of ketones and interaction analysis of engineered stereocomplementary ADHs. **(A)** *Pp*YSDR, **(B)** *Lf*SDR1, **(C)** RCR, **(D)** BaSDR1.

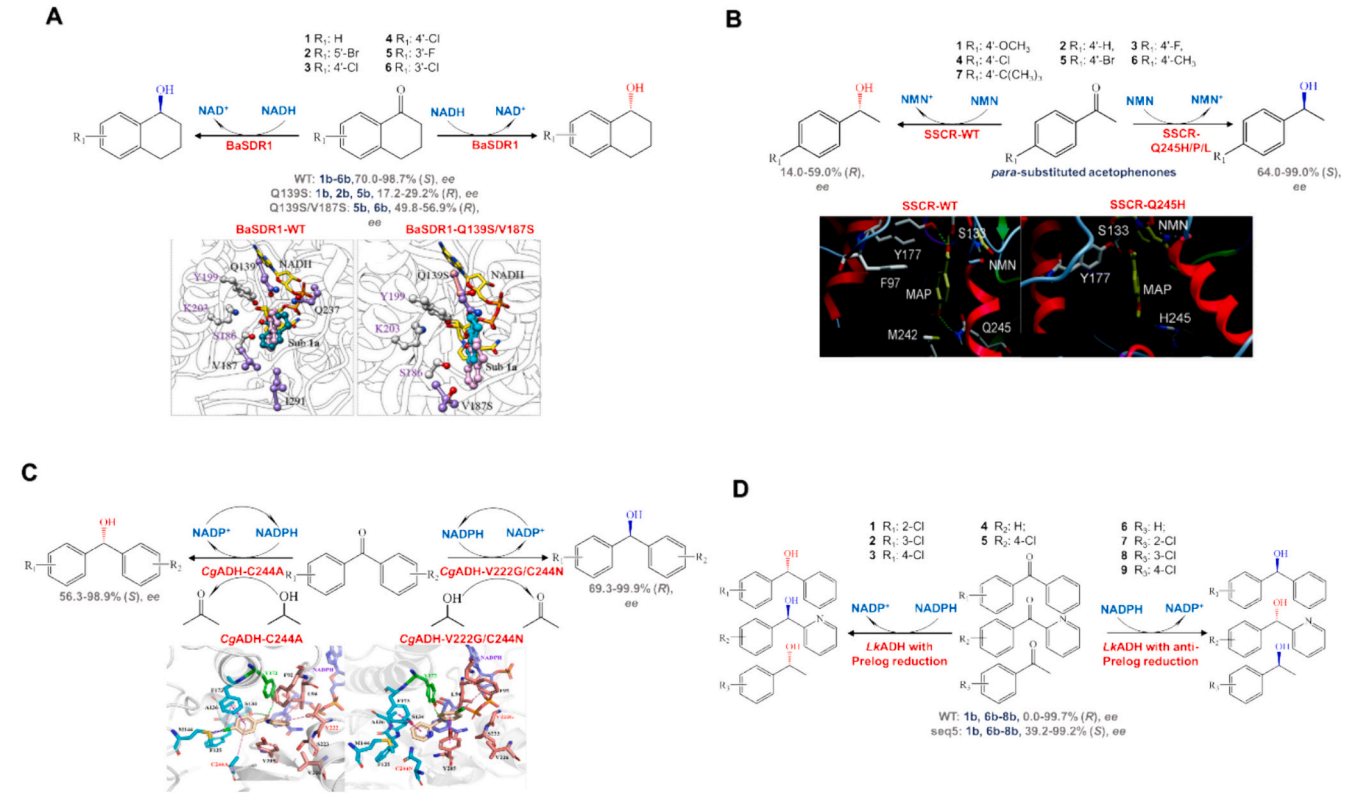

Fig. 6. Asymmetric reduction of ketones and interaction analysis of engineered stereocomplementary ADHs. **(A)** BaSDR1, **(B)** SSCR, **(C)** *Cg*ADH, **(D)** *Lk*ADH. **(F)** SSCR, **(G)** *Cg*ADH, **(H)** *Lk*ADH, **(I)** *Tt*ADH, **(J)** *Tb*SADH, **(K)** *Kp*ADH.

with 99 % *ee*, while the parent produced (*R*)- enantiomer in 99 % *ee* (Fig. 5C). This work suggests that the introduction of smaller residues could effectively enlarged the volume of small pocket to form a new large substrate binding pocket, which could accommodate the bulky aromatic substrates and lead to anti-Prelog stereoselectivity [68].

Carbonyl reductase (BaSDR1) was discovered by the genome hunting of *Bacillus aryabhattai* toward aromatic ketones and *β*-ketoesters. However, negligible activity was detected toward *β*-ketoesters. Based on the analysis of enzyme-substrate complex, bulky side chains of F250, Q237, Q242, and Q139 might be mainly responsible for insufficient space in accommodating ester group of *β*-ketoesters. Compared with the parent, structure-guided designed variant Q139G was obtained with significantly increased activity toward *β*-ketoesters. Importantly, Q139G displayed inverted stereoselectivity from Prelog to *anti*-Prelog with 89–99 % *ee* toward *β*-ketoesters, whereas the stereoselectivity toward aromatic ketones was unchanged. This study indicates that *anti*-Prelog-preferred carbonyl reductase can be achieved through adjusting the substrate binding mode by structure-guided redesign of substrate-binding pocket (Fig. 5D) [69].

In the engineering of BaSDR1, mutagenesis of residues affecting substrate binding was conducted to modulating their steric hindrance and hydrophobicity. Multiple mutants were obtained with improved catalytic efficiency and stereoselectivity (99 % *ee*). Variants Q139S and Q139S/V187S exhibited decreased or reversed *ee* values toward *α*-tetralone and derivatives. Further analysis indicates that the catalytic activity and stereoselectivity of BaSDR1 toward bulky ketones were improved through rational reconstruction of substrate binding pocket. The enlarger substrate cavity and changed hydrophobicity in variants allow different binding orientations and reversal of stereoselectivity (Fig. 6A) [46].

5.3. Reversed stereoselectivity of SSCR based on substrate interaction analysis

Carbonyl reductase from *Sporobolomyces salmonicolor* (SSCR) was identified with 14 %–59 % *ee* (*R*) toward *para*-substituted acetophenones. Molecular docking indicates that hydrogen bondings and hydrophobic interactions between residues Q245 and M242 and the substrates may be responsible for the low selectivity. Interestingly, single variants Q245H, Q245P, and Q245L with reversed *ee* values were obtained by saturation mutagenesis of Q245. Molecular docking shows that *para*-substituted acetophenone adopted an energetically preferred conformation of *re*-face in the active centers which was favorable for *pro-S* attack (Fig. 6B) [70].

5.4. Inverted stereoselectivity of CgADH by substrate docking and sequence alignment

Sun and coworkers identified a NADP(H)-dependent alcohol dehydrogenase *Cg*ADH from *C. glabrata* that exhibited dual activities of reducing and oxidizing. Based on multiple sequence alignment analysis, *Cg*ADH belongs to Extended-SDR subfamily. Through substrate docking and sequence alignment, two excellent variants, C244A and V222G/C244N, were obtained. C244A exhibited a 71-fold increase in catalytic efficiency toward CPMK, and improved stereoselectivity of 99 % (*R*) compared with 87 % (*R*) of its parent. Double variant V222G/C244N exhibited a 25-fold increase in catalytic efficiency toward CPMK with a completely reversed stereoselectivity of 95 % (*S*). The position of chlorine substitution on the phenyl ring significantly affects the catalytic activity and stereoselectivity of *Cg*ADH. The pyridine ring also plays important role in stereoselectivity (Fig. 6C) [61].

5.5. Inverted stereoselectivity of LkADH by "Shrinkage mutagenesis" approach

*Lk*ADH from *Lactobacillus kefiri* was engineered for increased activity and stereoselectivity toward 4-chlorodiphenylketones by Shao and coworkers. Based on substrate-enzyme complex, Tyr190 with the largest volume in the substrate binding pocket was chosen for saturation mutagenesis. Y190P exhibited the highest *ee* of 72 %, and was used as the template to perform further rounds of mutagenesis. Using focused libraries and "shrinkage mutagenesis" approach, variant seq5 was obtained with significantly enhanced activity and >99 % *ee* for the production of (*R*)-(4-chlorophenyl)-(phenyl)-methanol. Interestingly, seq5 also exhibited inverted *S*-stereopreference toward 2-chloro-1-phenylethanone and 3-chloro-1-phenylethanone. MD analysis shows that higher flexibility of 4-chlorodiphenylketones in enlarged binding cavity is favorable for *pro-R* pre-reaction conformation (Fig. 6D) [71].

5.6. Computational design of TtADH with inverted enantioselectivity

Strictly NAD(H)-dependent thermostable ketoreductases from *Thermus thermophilus* (*Tt*ADH) can catalyze the reduction of aromatic ketones and *α*-ketoesters following Prelog manner. A CASCO (catalytic selectivity by computational design) workflow including near-attack conformations (NACs) scoring and multiple short MD simulations for ranking was used to generate ADH mutants with *anti*-prolog preference. CASCO designed variants K1 (99% *ee*), K2 (92% *ee*) and K3 (93% *ee*) were generated with reversed *R*-enantioselectivity toward acetophenone and moderate expense of catalytic efficiency. Moreover, K1, K2 and K3 also exhibit inverted enantioselectivity toward trifluorinated and dichlorinated ketones with >90 % *ee*. Introduction of larger hydrophobic side chains in variants formed new interactions with substrates and resulted in substrate orientation toward the *pro-R* conformation (Fig. 7A) [45].

5.7. Triple-code saturation mutagenesis of TbSADH for inverted enantioselectivity

*Tb*SADH from *Thermoethanolicus brockii* is an attractive industrial biocatalyst because of its high thermostability. Using triple-code saturation mutagenesis (TCSM), two stereocomplementary variants SZ2074 (I86N/C295N) with *ee* value of 99 % (*R*) and SZ2172 (I86V/W110L/L294Q) with 95 % *ee* (*S*) were obtained. Deconvolution analysis indicates that residues at 294 and 295 are "switches" that specifically control the inversion of product chirality. Further MD simulations and quantum mechanics (QM) calculations reveal that the different hydrogen bonding interactions formed by 294 and 295 with the O atom of furan ring led to reversal of stereoselectivity (Fig. 7B) [72,73].

5.8. Inverted stereoselectivity of KpADH by HCSM and polarity scanning

Bulky-bulky ketone, CPMK, was regarded as "difficult-to-reduce" ketone. *Kp*ADH from *Kluyveromyces polyspora* was discovered by genome mining and showed high conversion ratio, however, only moderate *ee* value of 82 % (*R*) toward (4-chlorophenyl) (pyridine-2-yl) ketone (CPMK). To develop a "small but smart" library, hydroclassified combinatorial saturation mutagenesis (HCSM) strategy was proposed to engineer substrate binding pocket for improved stereoselectivity. Variant 50C10 (C165F/E214Y/S237A) was obtained with the highest *ee* of 99 %. More importantly, 50C10 also maintained high catalytic efficiency (k_{cat}/K_M = 16.9 s^{-1} mM^{-1}). 50C10 also displayed 88–99 % *ee* toward other diaryl ketones with large electron-withdrawing substituents at *para*-position. MD simulations demonstrate that the hydrophobic interactions with the substrate in the large substrate binding pocket and the altered steric hindrance in the small substrate binding pocket are the main factors for the enhanced stereoselectivity [74].

To gain deep insight into stereoselectivity of *Kp*ADH toward diaryl ketones, polarity scanning of the substrate binding pocket of *Kp*ADH was performed using asparagine and valine as polar/nonpolar sieves. Variants Mu-R2 with enhanced *ee* value of 99 % (*R*) and Mu-S5 with inverted *ee* value of 98 % (*S*) were obtained. Based on crystal structure and MD

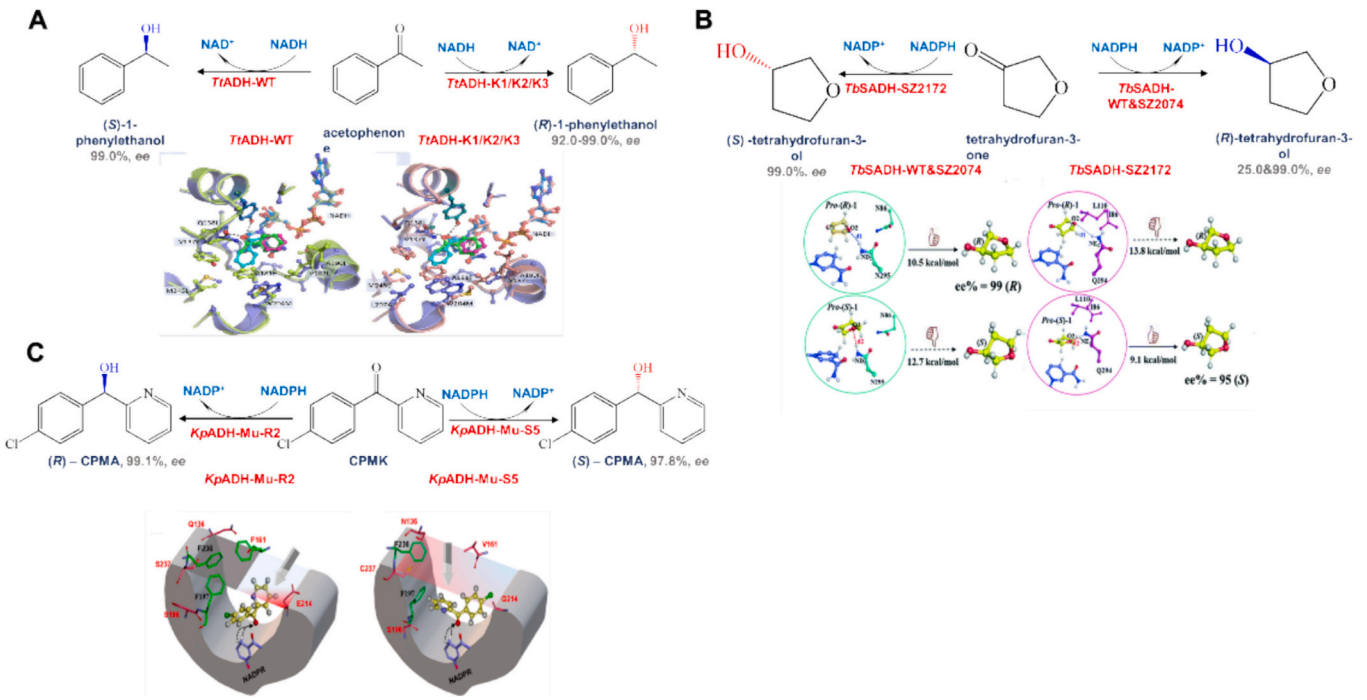

Fig. 7. Asymmetric reduction of ketones and interaction analysis of engineered stereocomplementary ADHs. **(A)** *Tt*ADH, **(B)** *Tb*SADH, **(C)** *Kp*ADH.

simulation, polarity change at the substrate entrance is responsible for the increased and inverted enantioselectivity of variants. The *pro-S* orientation of CPMK was defined when it passed through the "polar gate", a quadrilateral plane formed by α-carbons of four residues including N136, V161, C237, and G214, leading to a reversed enantiopreference of Mu-S5 (Fig. 7C) [44].

To further explore the determinants of CPMK stereoselectivity of *Kp*ADH, Zhang and coworkers conducted kinetics and interaction analysis on E214I/T215S/S237A with >99 % (*S*) and F161V/S196G/E214G with >99 % (*R*). The results indicate that the elimination of side-chain collisions and the enhancement of electrostatic interactions are crucial factors in improved catalytic efficiency and stereoselectivity. Moreover, mutation of E214 to a hydrophobic residue favored *pro-S* attack from *re*-face to form (*S*)-alcohols, while a hydrophilic mutation favored *pro-R* attack to generate (*R*)-alcohols [75].

6. Applications

Both enantiomers of alcohols serve as important chiral building blocks that can be used for the synthesis of various blockbuster drugs, such as atorvastatin (Lipitor), Montelukast (Singulair), Ibrutinib, and so on (Table 1) [76–78]. In recent years, asymmetric reduction catalyzed by ADHs has been intensively investigated for chiral alcohol synthesis due to excellent regioselectivity and stereoselectivity, high catalytic efficiency, and green environmental friendliness. Biocatalytic asymmetric reaction becomes the "*first-of-choice*" in the era of green chemistry and biomanufacturing. Increasing number of ADHs with different properties, stereoselectivity in especial, were developed in recent years. A number of ADH-catalyzed reactions have been successfully applied in industrial production [79–81].

Atorvastatin calcium is a blockbuster drug of Pfizer for the treatment of hypercholesterolemia and related cardiovascular diseases (Scheme 1). It can reduce the risk of cardiovascular disease by inhibiting enzymes involved in cholesterol biosynthesis. As a third-generation statin drug, it has a more significant therapeutic effect with fewer side effects. 6-Cyano-(3*R*,5*R*)-dihydroxyhexanoic acid tert-butyl ester, a key chiral intermediate for synthesizing Atorvastatin, has two chiral centers and four different enantiomers. ADHs has been used for the synthesis of 6-cyano-(3*R*,5*R*)-dihydroxyhexanoic acid tert-butyl ester with high optical purity chiral alcohol products. Under guidance of reaction-kinetic model-guided biocatalyst engineering strategy, the coupling efficiency of *Km*AKR from *Kluyveromyces marxianu* and *Bm*GDH was increased, resulting in high space-time yields (>1000 g/L d^{-1}) of *t*-butyl 6-cyano-(3*R*, 5*R*)-dihydroxyhexanoate in 50 L bioreactors [82].

Multiple ADHs have been commercialized, such as Codex® Ketoreductase (KRED) screening kit. Codexis successfully developed ADH biocatalyst to synthesize (*S*)-4-chloro-3-hydroxybutanoic acid ethyl ester [(*S*)-CHBE] from 4-chloro-3-oxobutanoic acid ethyl ester (COBE) [83]. Yang et al. employed *Sm*ADH31 from *Stenotrophomonas maltophilia* for asymmetric reduction, achieving complete conversion at 4.0 M COBE with >99 % *ee* [84]. *Dh*CR and *Cg*CR were also employed in asymmetric preparation of (*S*)- and (*R*)-CHBE with >99 % *ee* at 330 g/L COBE [59].

Irutinib belongs to a class of "tyrosine kinase inhibitors" commonly used in the treatment of adult lymphocytic leukemia, small lymphocytic lymphoma, Mantle cell lymphoma and macroglobulinemia through inhibiting the growth and spread of cancer cells and abnormal immune cells [85]. (*S*)- N-Boc-3-hydroxypiperidine ((*S*)-NBHP) is the key chiral intermediate for the synthesis of Irutinib [86]. Carbonyl reductase *Ch*KRED03 obtained through gene mining and could catalyze the asymmetric production of (*S*)-NBHP in 99 % *ee* at 200 g·L^{-1} NBPO [87]. Zheng et al. reported the rational engineering of *Cg*KR1 to obtain variant F92C/F94W with activity of 300 U·mg^{-1} and >99 % *ee* (*S*) toward NBPO [88]. *Kp*ADH could catalyze the reduction of NBPO to (*S*)-NBHP 97 % *ee*. Based on crystallization and molecular docking, Y127W with 8-fold increased catalytic efficiency and 99 % *ee* (*S*) was achieved [89]. As much as 600 g·L^{-1} NBPO could be completely reduced into (*S*)-NBHP.

Anti-Prelog-specific (*R*)-1-(4-hydroxyphenyl)-ethanol dehydrogenase [(*R*)-HPED] from *Aromatoleum aromaticum* belongs to the 'classical' family within SDR superfamily. Prelog-specific NADH-dependent (*S*)-selective 1-phenylethanol dehydrogenase from the denitrifying bacterium *A. aromaticum strain* EbN1 (*E. coli*/(*S*)-PED), was identified by Johann Heider. Biotransformations catalyzed by both enzymes, followed by TFA-catalyzed cyclization of the resulting γ-hydroxy esters, furnished the respective (*S*)- and (*R*)-configured products with exquisite optical purity (up to >99 % *ee*). In large-scale model compound methyl 4-oxo-4-phenylbutanoate asymmetric reduction reaction, Using one-pot

Table 1
Application of chiral alcohols as the key building blocks in drug synthesis.

Chiral alcohol structural formula	Prelog or *anti*-Prelog attack	Target drug
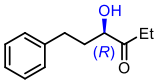	*anti*-Prelog attack	Benazepril [105]
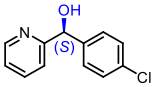	*anti*-Prelog attack	Bepotastine [74]
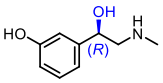	*anti*-Prelog attack	Phenylephrine [106]
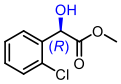	*anti*-Prelog attack	Clopidogrel [107]
	*anti*-Prelog attack	Talsaclidine [108]
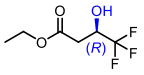	*anti*-Prelog attack	Befloxatone [109]
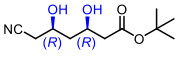	*anti*-Prelog attack	Atorvastatin calcium [110]
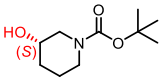	Prelog attack	Ibrutinib [4]
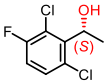	Prelog attack	Crizotinib [111]
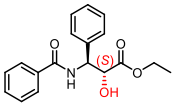	Prelog attack	Paclitaxel [112]
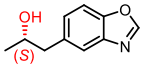	Prelog attack	Talampanel [113]
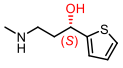	Prelog attack	Cymbalta [114]

two-step direct bioreduction-lactonization reaction sequence catalyzed by *E. coli*/(*S*)-PED biocatalysis and TFA-dependent chemical conversion, (*S*)-γ-phenyl-γ-butyrolactone (>99 % *ee*) in 67–74 % isolated yield at 89–95 % conversion was obtained [90–92].

In addition to asymmetric production of high-value chiral-alcohols, oxidative activity of ADH can also be used for producing valuable compounds [93,94]. Nootkatone, a compound naturally found in grapefruit peel, has multiple biological activities such as antioxidant, anti-cancer, anti-inflammatory, hypolipidemic, hypoglycemic, cardiovascular disease prevention, and can also be used as a natural food additive to enhance the flavor of citrus foods [95]. Cytochrome P450 BM3 and an ADH were applied to construct in vitro two-step oxidation of (+)-valencene to produce (+)-nootkatone [96].

Coenzymes (NADH, NADPH, FAD, CoA, etc.) act as reducing agents in numerous enzyme-catalyzed redox reactions, such as alkene reductases, monooxygenases, amino acid dehydrogenase, imine reductase, etc. Considering the instability and high price of reduced coenzymes, coenzyme recycling systems were applied for enzyme catalysis [97–99]. ADHs can generate reduced coenzymes when exerting oxidative activity, and their oxidative properties can be used in cofactor regeneration (Scheme 2). A propionaldehyde dehydrogenase was developed and variant M3 (R48L/N193T/K199Y) was obtained with improved activity and thermostability. [100]. M3 was used for cofactor recycling in asymmetric reduction amination of trimethylpyruvate. A biocatalytic redox cascade approach for one-pot deracemization of carboxyl-substituted tetrahydroisoquinolines was developed by Ju et al. [101]. (*S*)-tetrahydroisoquinoline carboxylic acid can be prepared through two-step process involving racemic resolution and asymmetric reduction. In asymmetric reduction reaction, the classic dehydrogenase *Tb*ADH was introduced as a cofactor recycling system. One-pot conversion of racemic tetrahydroisoquinoline carboxylic acid into single enantiomer (*S*)-tetrahydroisoquinoline carboxylic acid with conversion rates and *ee* value of over 99 % were achieved. Stereocomplementary ADHs has also been applied to control racemization of enantiopure phenyl-ring-containing secondary alcohols. Variant W110G of *Te*SADH from *Thermoanaerobacter pseudoethanolicus* catalyzed stereoselectively conversion of *R*-alcohols to *S*-alcohols via non-selective oxidation and *S*-selective reduction, in which 3 % (*v*/v) acetone and 30 % (v/v) 2-propanol were used to control the stereoselectivity of the oxidation and reduction reactions. [102].

7. Future perspectives

Natural *anti*-Prelog ADH is relatively rare and hard to be discovered from enzyme library. Based on structural and functional analysis of various ADHs, properties of residues surrounding the substrate binding pocket and volume of substrate binding pocket have been reported to be critical in the modulating of stereoselectivity. ADHs with improved or reversed stereoselectivity could be obtained by expanding or shrinking the substrate binding pocket based on steric hindrance. In addition, engineering of hydrogen bonding, ionic bonding, hydrophobic interaction, and π-π interaction between key residues and substrates is effective for the development of stereocomplementary ADHs.

Machine learning has been applied as an efficient computational-guided method in the field of enzyme engineering from scratch [103,104]. In subsequent efforts, stereocomplementary ADHs structure information and machine learning should be combined to predict variants with excellent stereoselectivity, thereby reducing the amount of workloads required for enzyme engineering and accelerating the development of desirable biocatalysts for biosynthesis of fine chemicals.

Artificial enzymes refer to use of artificial polymers in the mimetic

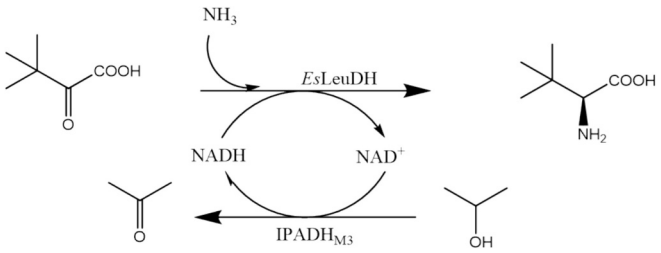

Scheme 2. Alcohol dehydrogenase used in the coenzyme cycle system.

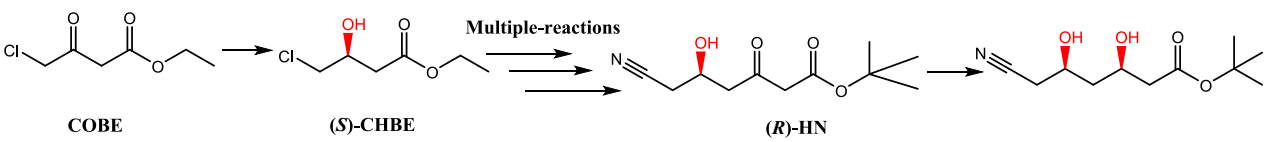

Scheme 1. The synthetic pathway of chiral alcohol building blocks for atorvastatin.

enzyme active center or introduce of chemically active atoms in a polymer-based scaffold. Elucidation of the origins of stereoselective catalytic mechanism of stereocomplementary alcohol dehydrogenases could deepen the understanding of enzyme catalysis and provide guidance for design of stereoselective artificial enzymes. Besides the key catalytic residues, other residues with appropriate properties could be rationally introduced to providing complementary shape, hydrogen bonding, ionic bonding, hydrophobic interaction, and π-π interaction with substrates, which will form stereoselective and efficient artificial active center. The development of artificial enzymes could accelerate the development of biocatalysts with desired properties for the synthesis of pharmaceuticals, agrochemicals, materials, fine chemical, etc.

8. Conclusion

This review presents an overview of classification, functional basis, and applications of stereocomplementary ADHs in agrochemical, pharmaceutical and chemical industries. Based on analysis of naturally evolved and tailor-made stereocomplementary ADHs, molecular mechanisms underlying stereoselectivity control toward non-natural substrates, such as dialkyl ketones and heterocyclic ketones have been unveiled. This review also summarizes rational design strategies, such as binding-pocket complementary mutation strategy by manipulating properties of substrate binding pockets, such as steric hindrance, enzyme-ligand interactions, for construction of variants with elevated and/or inverted stereoselectivity for synthesis of both enantiomers of secondary alcohols. This review could provide useful guidance for the engineering of ADHs with complementary *anti*-Prelog and Prelog selectivity for the biosynthesis of fine chemicals of industrial relevance.

Funding

This project was supported by the National Key Research and Development Program (2021YFC2102700), National Natural Science Foundation of China (22377040, 22378169) for the financial support of this research.

CRediT authorship contribution statement

Lu Zhang: Writing – original draft, Investigation. **Zewen Sun:** Writing – original draft, Investigation. **Guochao Xu:** Writing – review & editing, Funding acquisition, Conceptualization. **Ye Ni:** Writing – review & editing, Supervision, Funding acquisition, Conceptualization.

Declaration of competing interest

The authors declare that they have no known competing financial interests or personal relationships that could have appeared to influence the work reported in this paper.

Data availability

No data was used for the research described in the article.

References

[1] F. Hollmann, D.J. Opperman, C.E. Paul, Biocatalytic reduction reactions from a chemist's perspective, Angew. Chem. Int. Ed. Eng. 60 (11) (2021) 5644–5665, https://doi.org/10.1002/anie.202001876.
[2] A.A. Koesoema, D.M. Standley, T. Senda, T. Matsuda, Impact and relevance of alcohol dehydrogenase enantioselectivities on biotechnological applications, Appl. Microbiol. Biotechnol. 104 (7) (2020) 2897–2909, https://doi.org/10.1007/s00253-020-10440-2.
[3] G.A. Strohmeier, H. Pichler, O. May, M. Gruber-Khadjawi, Application of designed enzymes in organic synthesis, Chem. Rev. 111 (7) (2011) 4141–4164, https://doi.org/10.1021/cr100386u.
[4] X. Ying, J. Zhang, C. Wang, M. Huang, Y. Ji, F. Cheng, M. Yu, Z. Wang, M. Ying, Characterization of a carbonyl reductase from *Rhodococcus erythropolis* WZ010 and its variant Y54F for asymmetric synthesis of (*S*)-N-boc-3-hydroxypiperidine, Molecules 23 (12) (2018) 3117, https://doi.org/10.3390/molecules23123117.
[5] L. Qiao, Z. Luo, H. Chen, P.F. Zhang, A. Wang, R.A. Sheldon, Engineering ketoreductases for the enantioselective synthesis of chiral alcohols, Chem. Commun. (Camb.) 59 (49) (2023) 7518–7533, https://doi.org/10.1039/d3cc01474f.
[6] C.D.F. Milagre, H.M.S. Milagre, Alcohol dehydrogenase-catalyzed oxidation, Curr. Opin. Green Sustain. Chem. 10 (38) (2022), https://doi.org/10.1016/j.cogsc.2022.100694.
[7] Z. Li, H. Yang, J. Liu, Z.D. Huang, F. Chen, Application of ketoreductase in asymmetric synthesis of pharmaceuticals and bioactive molecules: an update (2018-2020), Chem. Rec. 21 (7) (2021) 1611–1630, https://doi.org/10.1002/tcr.202100062.
[8] A. Chadha, S.K. Padhi, S. Stella, S. Venkataraman, T. Saravanan, Microbial alcohol dehydrogenases: recent developments and applications in asymmetric synthesis, Org. Biomol. Chem. 22 (2) (2024) 228–251, https://doi.org/10.3390/microorganisms12020311.
[9] A.S. de Miranda, C.D.F. Milagre, F. Hollmann, Alcohol dehydrogenases as catalysts in organic synthesis, Front. Catal. 2 (2022), https://doi.org/10.3389/fctls.2022.900554.
[10] X. Chen, Z. Dou, T. Luo, Z. Sun, H. Ma, G. Xu, Y. Ni, Directed reconstruction of a novel ancestral alcohol dehydrogenase featuring shifted pH-profile, enhanced thermostability and expanded substrate spectrum, Bioresour. Technol. 363 (2022) 127886, https://doi.org/10.1016/j.biortech.2022.127886.
[11] L. Zhang, W. Dai, S. Rong, G.C. Xu, Y. Ni, Engineering diaryl alcohol dehydrogenase *Kp*ADH reveals importance of retaining hydration shell in organic solvent tolerance, Protein Sci. 33 (4) (2024) e4933, https://doi.org/10.1002/pro.4933.
[12] A.S. de Miranda, C.D.F. Milagre, F. Hollmann, Alcohol dehydrogenases as catalysts in organic synthesis, Front. Catal. 2 (2022) 900554, https://doi.org/10.3389/fctls.2022.900554.
[13] J. Zhou, G. Xu, Y. Ni, Stereochemistry in asymmetric reduction of bulky–bulky ketones by alcohol dehydrogenases, ACS Catal. 10 (19) (2020) 10954–10966, https://doi.org/10.1021/acscatal.0c02646.
[14] A.E. Sardauna, M. Abdulrasheed, A. Nzila, M.M. Musa, Biocatalytic asymmetric reduction of prochiral bulky-bulky ketones, Mol. Catal. 541 (2023) 113099, https://doi.org/10.1016/j.mcat.2023.113099.
[15] M.M. Musa, Alcohol dehydrogenases with anti-Prelog stereopreference in synthesis of enantiopure alcohols, ChemistryOpen 11 (4) (2022) e202100251, https://doi.org/10.1002/open.202100251.
[16] J. An, Y. Nie, Y. Xu, Structural insights into alcohol dehydrogenases catalyzing asymmetric reductions, Crit. Rev. Biotechnol. 39 (3) (2019) 366–379, https://doi.org/10.1080/07388551.2019.1566205.
[17] A.P. Shanbhag, Stairway to stereoisomers: engineering short- and medium-chain ketoreductases to produce chiral alcohols, ChemBioChem 24 (6) (2023) e202200687, https://doi.org/10.1002/cbic.202200687.
[18] M.M. Musa, R.S. Phillips, Recent advances in alcohol dehydrogenase-catalyzed asymmetric production of hydrophobic alcohols, Catal. Sci. Technol. 1 (8) (2011) 1311–1323, https://doi.org/10.1039/c1cy00160d.
[19] T.M. Penning, The aldo-keto reductases (AKRs): overview, Chem. Biol. Interact. 234 (2015) 236–246, https://doi.org/10.1016/j.cbi.2014.09.024.
[20] S. Kamitori, A. Iguchi, A. Ohtaki, M. Yamada, K. Kita, X-ray structures of NADPH-dependent carbonyl reductase from *Sporobolomyces salmonicolor* provide insights into stereoselective reductions of carbonyl compounds, J. Mol. Biol. 352 (3) (2005) 551–558, https://doi.org/10.1016/j.jmb.2005.07.011.
[21] Y. Kallberg, U. Oppermann, B. Persson, Classification of the short-chain dehydrogenase/reductase superfamily using hidden Markov models, FEBS J. 277 (10) (2010) 2375–2386, https://doi.org/10.1111/j.1742-4658.2010.07656.x.
[22] P.C. Guo, Z.Z. Bao, X.X. Ma, Q. Xia, W.F. Li, Structural insights into the cofactor-assisted substrate recognition of yeast methylglyoxal/isovaleraldehyde reductase Gre2, Biochim. Biophys. Acta 1844 (9) (2014) 1486–1492, https://doi.org/10.1016/j.bbapap.2014.05.008.
[23] K.L. Kavanagh, H. Jornvall, B. Persson, U. Oppermann, Medium- and short-chain dehydrogenase/reductase gene and protein families: the SDR superfamily: functional and structural diversity within a family of metabolic and regulatory enzymes, Cell. Mol. Life Sci. 65 (24) (2008) 3895–3906, https://doi.org/10.1007/s00018-008-8588-y.
[24] A.M. Lesk, NAD-binding domains of dehydrogenases, Curr. Opin. Struct. Biol. 5 (6) (1995) 775–783, https://doi.org/10.1016/0959-440x(95)80010-7.
[25] C. Filling, K.D. Berndt, J. Benach, S. Knapp, T. Prozorovski, E. Nordling, R. Ladenstein, H. Jornvall, U. Oppermann, Critical residues for structure and catalysis in short-chain dehydrogenases/reductases, J. Biol. Chem. 277 (28) (2002) 25677–25684, https://doi.org/10.1074/jbc.M202160200.
[26] A. Koumanov, J. Benach, S. Atrian, R. Gonzalez-Duarte, A. Karshikoff, R. Ladenstein, The catalytic mechanism of *Drosophila* alcohol dehydrogenase: evidence for a proton relay modulated by the coupled ionization of the active site lysine/tyrosine pair and a NAD+ ribose OH switch, Proteins 51 (2) (2003) 289–298, https://doi.org/10.1002/prot.10354.
[27] H. Man, S. Gargiulo, A. Frank, F. Hollmann, G. Grogan, Structure of the NADH-dependent thermostable alcohol dehydrogenase TADH from *Thermus* sp. ATN1 provides a platform for engineering specificity and improved compatibility with inorganic cofactor-regeneration catalysts, J. Mol. Catal. B Enzym. 105 (2014) 1–6, https://doi.org/10.1016/j.molcatb.2014.03.013.
[28] P.J. Baker, K.L. Britton, M. Fisher, J. Esclapez, C. Pire, M.J. Bonete, J. Ferrer, D. W. Rice, Active site dynamics in the zinc-dependent medium chain alcohol

dehydrogenase superfamily, Proc. Natl. Acad. Sci. USA 106 (3) (2009) 779–784, https://doi.org/10.1073/pnas.0807529106.
[29] H. Jornvall, J. Hedlund, T. Bergman, Y. Kallberg, E. Cederlund, B. Persson, Origin and evolution of medium chain alcohol dehydrogenases, Chem. Biol. Interact. 202 (1–3) (2013) 91–96, https://doi.org/10.1016/j.cbi.2012.11.008.
[30] J. Hedlund, H. Jornvall, B. Persson, Subdivision of the MDR superfamily of medium-chain dehydrogenases/reductases through iterative hidden Markov model refinement, BMC Bioinform. 11 (2010) 534, https://doi.org/10.1186/1471-2105-11-534.
[31] H. Jornvall, J. Hedlund, T. Bergman, U. Oppermann, B. Persson, Superfamilies SDR and MDR: from early ancestry to present forms. Emergence of three lines, a Zn-metalloenzyme, and distinct variabilities, Biochem. Biophys. Res. Commun. 396 (1) (2010) 125–130, https://doi.org/10.1016/j.bbrc.2010.03.094.
[32] A.J. Lapthorn, X. Zhu, E.M. Ellis, The diversity of microbial aldo/keto reductases from *Escherichia coli* K12, Chem. Biol. Interact. 202 (1–3) (2013) 168–177, https://doi.org/10.1016/j.cbi.2012.10.008.
[33] A.H. Ehrensberger, D.K. Wilson, Structural and catalytic diversity in the two family 11 aldo-keto reductases, J. Mol. Biol. 337 (3) (2004) 661–673, https://doi.org/10.1016/j.jmb.2004.01.059.
[34] F.X. Ruiz, A. Cousido-Siah, A. Mitschler, J. Farres, X. Pares, A. Podjarny, X-ray structure of the V301L aldo-keto reductase 1B10 complexed with NADP(+) and the potent aldose reductase inhibitor fidarestat: implications for inhibitor binding and selectivity, Chem. Biol. Interact. 202 (1–3) (2013) 178–185, https://doi.org/10.1016/j.cbi.2012.12.013.
[35] K. Yamamoto, D.K. Wilson, Identification, characterization, and crystal structure of an aldo-keto reductase (AKR2E4) from the silkworm *Bombyx mori*, Arch. Biochem. Biophys. 538 (2) (2013) 156–163, https://doi.org/10.1016/j.abb.2013.08.018.
[36] R. Kratzer, D.K. Wilson, B. Nidetzky, B. Nidetzky, Catalytic mechanism and substrate selectivity of aldo-keto reductases: insights from structure-function studies of *Candida tenuis xylose* reductase, IUBMB Life 58 (9) (2006) 499–507, https://doi.org/10.1080/15216540600818143.
[37] T.M. Penning, J.E. Drury, Human aldo-keto reductases: function, gene regulation, and single nucleotide polymorphisms, Arch. Biochem. Biophys. 464 (2) (2007) 241–250, https://doi.org/10.1016/j.abb.2007.04.024.
[38] Y. Ni, C.X. Li, H.M. Ma, J. Zhang, J.H. Xu, Biocatalytic properties of a recombinant aldo-keto reductase with broad substrate spectrum and excellent stereoselectivity, Appl. Microbiol. Biotechnol. 89 (4) (2011) 1111–1118, https://doi.org/10.1007/s00253-010-2941-4.
[39] D. Zhu, L. Hua, How carbonyl reductases control stereoselectivity: approaching the goal of rational design, Pure Appl. Chem. 82 (1) (2010) 117–128, https://doi.org/10.1351/pac-con-09-01-03.
[40] J. Cieslak, Cahn, Ingold Prelog's specification of asymmetric configuration in organic chemistry, Postepy Biochem. 7 (1961) 475–498.
[41] P. Liang, B. Qin, M. Mu, X. Zhang, X. Jia, S. You, Prelog and anti-Prelog stereoselectivity of two ketoreductases from *Candida glabrata*, Biotechnol. Lett. 35 (9) (2013) 1469–1473, https://doi.org/10.1007/s10529-013-1228-0.
[42] B.M. Su, Z.H. Shao, A.P. Li, M. Naeem, J. Lin, L.D. Ye, H.W. Yu, Rational design of dehydrogenase/reductases based on comparative structural analysis of prereaction-state and free-state simulations for efficient asymmetric reduction of bulky aryl ketones, ACS Catal. 10 (1) (2019) 864–876, https://doi.org/10.1021/acscatal.9b04778.
[43] F. Qin, B. Qin, W. Zhang, Y. Liu, X. Su, T. Zhu, J. Ouyang, J. Guo, Y. Li, F. Zhang, J. Tang, X. Jia, S. You, Discovery of a switch between Prelog and anti-Prelog reduction toward halogen-substituted acetophenones in short-chain dehydrogenase/reductases, ACS Catal. 8 (7) (2018) 6012–6020, https://doi.org/10.1021/acscatal.8b00807.
[44] J. Zhou, Y. Wang, G. Xu, L. Wu, R. Han, U. Schwaneberg, Y. Rao, Y.L. Zhao, J. Zhou, Y. Ni, Structural insight into enantioselective inversion of an alcohol dehydrogenase reveals a "polar gate" in stereorecognition of diaryl ketones, J. Am. Chem. Soc. 140 (39) (2018) 12645–12654, https://doi.org/10.1021/jacs.8b08640.
[45] E. Delgado-Arciniega, H.J. Wijma, C. Hummel, D.B. Janssen, Computationally supported inversion of ketoreductase stereoselectivity, ChemBioChem 24 (9) (2023) e202300032, https://doi.org/10.1002/cbic.202300032.
[46] A. Li, W. Ting, K. Yang, X. Zhang, D. Yin, Y. Qin, L. Zhang, Engineering a carbonyl reductase as a potential tool for the synthesis of chiral α-tetralinols, ChemCatChem 13 (21) (2021) 4625–4633, https://doi.org/10.1002/cctc.202100890.
[47] H. Li, D. Zhu, L. Hua, E.R. Biehl, Enantioselective reduction of diaryl ketones catalyzed by a carbonyl reductase from *Sporobolomyces salmonicolor* and its mutant enzymes, Adv. Synth. Catal. 351 (4) (2009) 583–588, https://doi.org/10.1002/adsc.200900045.
[48] X.A. Shi, H.H. Lin, X.P. Wang, S.Y. Fang, Relationship between alcohol dehydrogenase isoenzyme gene expression and the catalytic asymmetric reduction of 2-Octanone by *Saccharomyces cerevisiae*, Chin. J. Process. Eng. 17 (4) (2017) 7, https://doi.org/10.12034/j.issn.1009-606X.216350.
[49] A. Yamashita, M. Endo, T. Higashi, T. Nakatsu, Y. Yamada, J. Oda, H. Kato, Capturing enzyme structure prior to reaction initiation: tropinone reductase-II-substrate complexes, Biochemistry 42 (19) (2003) 5566–5573, https://doi.org/10.1021/bi0272712.
[50] K. Nakajima, A. Yamashita, H. Akama, T. Nakatsu, H. Kato, T. Hashimoto, J. Oda, Y. Yamada, Crystal structures of two tropinone reductases: different reaction stereospecificities in the same protein fold, PNAS 95 (9) (1998) 4876–4881, https://doi.org/10.1073/pnas.95.9.4876.
[51] A. Yamashita, K. Nakajima, H. Kato, T. Hashimoto, Y. Yamada, J. Oda, Crystallization and preliminary crystallographic study of tropinone reductase II from *Datura stramonium*, Acta Crystallogr. D Biol. Crystallogr. 54 (Pt 6 Pt 2) (1998) 1405–1407, https://doi.org/10.1107/s0907444998005782.
[52] K. Nakajima, H. Kato, J. Oda, Y. Yamada, T. Hashimoto, Site-directed mutagenesis of putative substrate-binding residues reveals a mechanism controlling the different stereospecificities of two tropinone reductases, J. Biol. Chem. 274 (23) (1999) 16563–16568, https://doi.org/10.1074/jbc.274.23.16563.
[53] A. Yamashita, H. Kato, S. Wakatsuki, T. Tomizaki, T. Nakatsu, K. Nakajima, T. Hashimoto, Y. Yamada, J. Oda, Structure of tropinone reductase-II complexed with NADP and pseudotropine at 1.9 Å resolution: implication for stereospecific substrate binding and catalysis, Biochemistry 38 (24) (1999) 7630–7637, https://doi.org/10.1021/bi9825044.
[54] D.D. Clark, J.M. Boyd, S.A. Ensign, The stereo selectivity and catalytic properties of 2-[(*R*)-2-Hydroxypropylthio]ethanesulfonate dehydrogenase are controlled by interactions between C-terminal arginine residues and the sulfonate of coenzyme M, Biochemistry 43 (21) (2004) 6763–6771, https://doi.org/10.1021/bi049783h.
[55] J.W. Bakelar, D.A. Sliwa, S.J. Johnson, Crystal structures of *S*-HPCDH reveal determinants of stereospecificity for *R*- and *S*-hydroxypropyl-coenzyme M dehydrogenases, Arch. Biochem. Biophys. 533 (1–2) (2013) 62–68, https://doi.org/10.1016/j.abb.2013.02.017.
[56] A.M. Krishnakumar, B.P. Nocek, D.D. Clark, S.A. Ensign, J.W. Peters, Structural basis for stereoselectivity in the (*R*)- and (*S*)-hydroxypropylthioethanesulfonate dehydrogenases, Biochemistry 45 (29) (2006) 8831–8840, https://doi.org/10.1021/bi0603569.
[57] D.A. Sliwa, A.M. Krishnakumar, J.W. Peters, S.A. Ensign, Molecular basis for enantioselectivity in the (*R*)- and (*S*)-hydroxypropylthioethanesulfonate dehydrogenases, a unique pair of stereoselective short-chain dehydrogenases/reductases involved in aliphatic epoxide carboxylation, Biochemistry 49 (16) (2010) 3487–3498, https://doi.org/10.1021/bi100294m.
[58] G.C. Xu, H.L. Yu, Y.P. Shang, J.H. Xu, Enantioselective bioreductive preparation of chiral halohydrins employing two newly identified stereocomplementary reductases, RSC Adv. 5 (29) (2015) 22703–22711, https://doi.org/10.1039/c4ra16779a.
[59] G.C. Xu, H.L. Yu, Z.J. Zhang, J.H. Xu, Stereocomplementary bioreduction of β-ketonitrile without ethylated byproduct, Org. Lett. 15 (21) (2013) 5408–5411, https://doi.org/10.1021/ol402733y.
[60] G. Xu, Y. Zhang, Y. Wang, Y. Ni, Genome hunting of carbonyl reductases from *Candida glabrata* for efficient preparation of chiral secondary alcohols, Bioresour. Technol. 247 (2018) 553–560, https://doi.org/10.1016/j.biortech.2017.09.111.
[61] Z.W. Sun, J.C. Zhang, D.J. Yin, G.C. Xu, Y. Ni, Novel alcohol dehydrogenase *Cg*ADH from *Candida glabrata* for stereocomplementary reduction of bulky-bulky ketones featuring self-sufficient NADPH regeneration, ACS Sustain. Chem. Eng. 10 (41) (2022) 13722–13732, https://doi.org/10.1021/acssuschemeng.2c03872.
[62] L. Yang, Y. Zhang, Y. Liu, H. Wang, D. Wei, Highly efficient synthesis of pharmaceutically relevant chiral 3-N-substituted-azacyclic alcohols using two enantiocomplementary short chain dehydrogenases, Biochem. Eng. J. 178 (2022) 108300, https://doi.org/10.1016/j.bej.2021.108300.
[63] T. Shanati, C. Lockie, L. Beloti, G. Grogan, M.B. Ansorge-Schumacher, Two enantiocomplementary ephedrine dehydrogenases from *Arthrobacter* sp. TS-15 with broad substrate specificity, ACS Catal. 9 (7) (2019) 6202–6211, https://doi.org/10.1021/acscatal.9b00621.
[64] T. Barcellos, K. Tauber, W. Kroutil, L.H. Andrade, Stereocomplementary asymmetric bioreduction of boron-containing ketones mediated by alcohol dehydrogenases, Tetrahedron-Asymmetry 22 (18–19) (2011) 1772–1777, https://doi.org/10.1016/j.tetasy.2011.10.012.
[65] U.T. Bornscheuer, G.W. Huisman, R.J. Kazlauskas, S. Lutz, J.C. Moore, K. Robins, Engineering the third wave of biocatalysis, Nature 485 (7397) (2012) 185–194, https://doi.org/10.1038/nature11117.
[66] H. Cui, K.E. Jaeger, M.D. Davari, U. Schwaneberg, CompassR yields highly organic-solvent-tolerant enzymes through recombination of compatible substitutions, Chem. Eur. J. 27 (8) (2021) 2789–2797, https://doi.org/10.1002/chem.202004471.
[67] A. Li, L. Ye, X. Yang, C. Yang, J. Gu, H. Yu, Structure-guided stereoselectivity inversion of a short-chain dehydrogenase/reductase towards halogenated acetophenones, Chem. Commun. (Camb.) 52 (37) (2016) 6284–6287, https://doi.org/10.1039/c6cc00051g.
[68] S. Wang, Y. Nie, Y. Xu, R. Zhang, T.P. Ko, C.H. Huang, H.C. Chan, R.T. Guo, R. Xiao, Unconserved substrate-binding sites direct the stereoselectivity of medium-chain alcohol dehydrogenase, Chem. Commun. (Camb.) 50 (58) (2014) 7770–7772, https://doi.org/10.1039/c4cc01752h.
[69] A. Li, T. Wang, Q. Tian, X. Yang, D. Yin, Y. Qin, L. Zhang, Single-point mutant inverts the stereoselectivity of a carbonyl reductase toward β-ketoesters with enhanced activity, Chem. Eur. J. 27 (20) (2022) 6283–6294, https://doi.org/10.1002/chem.202005195.
[70] D. Zhu, Y. Yang, S. Majkowicz, T.H. Pan, K. Kantardjieff, L. Hua, Inverting the enantioselectivity of a carbonyl reductase via substrate-enzyme docking-guided point mutation, Org. Lett. 10 (4) (2008) 525–528, https://doi.org/10.1021/ol702638j.
[71] K. Wu, Z. Yang, X. Meng, R. Chen, J. Huang, L. Shao, Engineering an alcohol dehydrogenase with enhanced activity and stereoselectivity toward diaryl ketones: reduction of steric hindrance and change of the stereocontrol element, Catal. Sci. Technol. 10 (6) (2020) 1650–1660, https://doi.org/10.1039/c9cy02444a.

[72] Z. Sun, R. Lonsdale, A. Ilie, G. Li, J. Zhou, M.T. Reetz, Catalytic asymmetric reduction of difficult-to-reduce ketones: triple-code saturation mutagenesis of an alcohol dehydrogenase, ACS Catal. 6 (3) (2016) 1598–1605, https://doi.org/10.1021/acscatal.5b02752.
[73] Y. Jiang, G. Qu, X. Sheng, F. Tong, Z. Sun, Unraveling the mechanism of enantio-controlling switches of an alcohol dehydrogenase toward sterically small ketone, Catal. Sci. Technol. 12 (6) (2022) 1777–1787, https://doi.org/10.1039/d2cy00031h.
[74] G.C. Xu, Y. Wang, M.H. Tang, J.Y. Zhou, J. Zhao, R.Z. Han, Y. Ni, Hydroclassified combinatorial saturation mutagenesis: reshaping substrate binding pockets of *Kp*ADH for enantioselective reduction of bulky–bulky ketones, ACS Catal. 8 (9) (2018) 8336–8345, https://doi.org/10.1021/acscatal.8b02286.
[75] J. Zhang, J. Zhou, G. Xu, Y. Ni, Stereodivergent evolution of *Kp*ADH for the asymmetric reduction of diaryl ketones with *para*-substituents, Mol. Catal. 524 (2022) 112315, https://doi.org/10.1016/j.mcat.2022.112315.
[76] G. Hughes, J.C. Lewis, Introduction: biocatalysis in industry, Chem. Rev. 118 (1) (2018) 1–3, https://doi.org/10.1021/acs.chemrev.7b00741.
[76] R.A. Sheldon, J.M. Woodley, Role of biocatalysis in sustainable chemistry, Chem. Rev. 118 (2) (2018) 801–838, https://doi.org/10.1021/acs.chemrev.7b00203.
[78] M. Hall, A.S. Bommarius, Enantioenriched compounds via enzyme-catalyzed redox reactions, Chem. Rev. 111 (7) (2011) 4088–4110, https://doi.org/10.1021/cr200013.
[79] N. Adebar, H. Groger, Flow process for ketone reduction using a superabsorber-immobilized alcohol dehydrogenase from *Lactobacillus brevis* in a packed-bed reactor, Bioengineering-Basel 6 (4) (2019) 99, https://doi.org/10.3390/bioengineering6040099.
[80] S. Yu, H. Li, Y. Lu, G. Zheng, A catalyst from *Burkholderia cenocepacia* for efficient anti-Prelog's bioreduction of 3,5-bis(trifluoromethyl) acetophenone, Appl. Biochem. Biotechnol. 184 (4) (2018) 1319–1331, https://doi.org/10.1007/s12010-017-2628-8.
[81] H. Ma, L. Yang, Y. Ni, J. Zhang, C.X. Li, G.W. Zheng, H. Yang, J.H. Xu, Stereospecific reduction of methyl o-chlorobenzoylformate at 300 g·L^{-1} without additional cofactor using a carbonyl reductase mined from *Candida glabrata*, Adv. Synth. Catal. 354 (9) (2012) 1765–1772, https://doi.org/10.1002/adsc.201100366.
[82] F. Cheng, S.Y. Zhou, L.X. Chen, W. Zhang, S.F. Li, C.Y. Weng, Y.J. Wang, Y. G. Zheng, Reaction-kinetic model-guided biocatalyst engineering for dual-enzyme catalyzed bioreaction system, Chem. Eng. J. 452 (2023) 138997, https://doi.org/10.1016/j.cej.2022.138997.
[83] T. Kaliaperumal, S.N. Gummadi, A. Chadha, Synthesis of both enantiomers of ethyl-4-chloro-3-hydroxbutanoate from a prochiral ketone using *Candida parapsilosis* ATCC 7330, Tetrahedron-Asymmetry 22 (14–15) (2011) 1548–1552, https://doi.org/10.1016/j.tetasy.2011.08.009.
[84] Z. Yang, W. Ye, Y. Xie, Q. Liu, R. Chen, H. Wang, D. Wei, Efficient asymmetric synthesis of ethyl (*S*)-4-chloro-3-hydroxybutyrate using alcohol dehydrogenase *Sm*ADH31 with high tolerance of substrate and product in a monophasic aqueous system, Org. Process. Res. Dev. 24 (6) (2020) 1068–1076, https://doi.org/10.1021/acs.oprd.0c00088.
[85] J.A. Burger, Targeting the microenvironment in chronic lymphocytic leukemia is changing the therapeutic landscape, Curr. Opin. Oncol. 24 (6) (2012) 643–649, https://doi.org/10.1097/CCO.0b013e3283589950.
[86] D.L. Hughes, Patent review of manufacturing routes to recently approved oncology drugs: ibrutinib, cobimetinib, and alectinib, Org. Process. Res. Dev. 20 (11) (2016) 1855–1869, https://doi.org/10.1021/acs.oprd.6b00304.
[87] G.P. Xu, H.B. Wang, Z.L. Wu, Efficient bioreductive production of (*S*)-N-Boc-3-hydroxypiperidine using ketoreductase ChKRED03, Process Biochem. 51 (7) (2016) 881–885, https://doi.org/10.1016/j.procbio.2016.04.008.
[88] G.W. Zheng, Y.Y. Liu, Q. Chen, L. Huang, H.L. Yu, W.Y. Lou, C.X. Li, Y.P. Bai, A. T. Li, J.H. Xu, Preparation of structurally diverse chiral alcohols by engineering ketoreductase *Cg*KR1, ACS Catal. 7 (10) (2017) 7174–7181, https://doi.org/10.1021/acscatal.7b01933.
[89] Y. Wu, J. Zhou, J. Ni, C. Zhu, Z. Sun, G. Xu, Y. Ni, Engineering an alcohol dehydrogenase from *Kluyveromyces polyspora* for efficient synthesis of ibrutinib intermediate, Adv. Synth. Catal. 364 (2) (2021) 332–340, https://doi.org/10.1002/adsc.202001313.
[90] I. Busing, H.W. Hoffken, M. Breuer, L. Wöhlbrand, B. Hauer, R. Rabus, Molecular genetic and crystal structural analysis of 1-(4-hydroxyphenyl)-ethanol dehydrogenase from '*Aromatoleum aromaticum*' EbN1, J. Mol. Microbiol. Biotechnol. 25 (5) (2015) 327–339, https://doi.org/10.1159/000439113.
[91] H.W. Hoffken, M. Duong, T. Friedrich, M. Breuer, B. Hauer, R. Reinhardt, R. Rabus, J. Heider, Crystal structure and enzyme kinetics of the (S)-specific 1-phenylethanol dehydrogenase of the denitrifying bacterium strain EbN1, Biochemistry 45 (1) (2006) 82–93, https://doi.org/10.1021/bi051596b.
[92] P. Borowiecki, N. Telatycka, M. Tataruch, A. Żądło-Dobrowolska, T. Reiter, K. Schühle, J. Heider, M. Szaleniec, W. Kroutil, Biocatalytic asymmetric reduction of γ-keto esters to access optically active γ-aryl-γ-butyrolactones, Adv. Synth. Catal. 362 (10) (2020) 2012–2029, https://doi.org/10.1002/adsc.201901483.
[93] H. Sato, R. Yamada, Y. Watanabe, T. Kiryu, S. Kawano, M. Shizuma, H. Kawasaki, Deracemization of 1-phenylethanols in a one-pot process combining Mn-driven oxidation with enzymatic reduction utilizing a compartmentalization technique, RSC Adv. 12 (17) (2022) 10619–10624, https://doi.org/10.1039/d2ra01326f.
[94] S.A. Nafiu, M. Takahashi, E. Takahashi, S.M. Hamdan, M.M. Musa, Simultaneous cyclic deracemisation and stereoinversion of alcohols using orthogonal biocatalytic oxidation and reduction reactions, Catal. Sci. Technol. 10 (24) (2020) 8213–8218, https://doi.org/10.1039/d0cy01524e.
[95] Y. Gou, F. Zhang, Y. Tang, C. Jiang, G. Bai, H. Xie, M. Chen, Z. Liao, Engineering nootkatone biosynthesis in *Artemisia annua*, ACS Synth. Biol. 10 (5) (2021) 957–963, https://doi.org/10.1021/acssynbio.1c00016.
[96] A. Kokorin, V.B. Urlacher, Artificial fusions between P450 BM3 and an alcohol dehydrogenase for efficient (+)-nootkatone production, ChemBioChem 23 (12) (2022) e202200065, https://doi.org/10.1002/cbic.202200065.
[97] Z. Yang, H. Fu, W. Ye, Y. Xie, Q. Liu, H. Wang, D. Wei, Efficient asymmetric synthesis of chiral alcohols using high 2-propanol tolerance alcohol dehydrogenase *Sm*ADH2 via an environmentally friendly TBCR system, Catal. Sci. Technol. 10 (1) (2021) 70–78, https://doi.org/10.1039/c9cy01794a.
[98] S. Kara, D. Spickermann, J.H. Schrittwieser, C. Leggewie, W.J.H. van Berkel, I.W. C.E. Arends, F. Hollmann, More efficient redox biocatalysis by utilising 1,4-butanediol as a 'smart cosubstrate', Green Chem. 15 (2) (2013) 330–335, https://doi.org/10.1039/c2gc36797a.
[99] R.D. Franklin, J.A. Whitley, A.A. Caparco, B.R. Bommarius, J.A. Champion, A. S. Bommarius, Continuous production of a chiral amine in a packed bed reactor with co-immobilized amine dehydrogenase and formate dehydrogenase, Chem. Eng. J. 407 (2021) 127065, https://doi.org/10.1016/j.cej.2020.127065.
[100] Q. Jia, Y.C. Zheng, H.P. Li, X.L. Qian, Z.J. Zhang, J.H. Xu, Engineering isopropanol dehydrogenase for efficient regeneration of nicotinamide cofactors, Appl. Environ. Microbiol. 88 (9) (2022) e0034122, https://doi.org/10.1128/aem.00341-22.
[101] S. Ju, M. Qian, J. Li, G. Xu, L. Yang, J. Wu, A biocatalytic redox cascade approach for one-pot deracemization of carboxyl-substituted tetrahydroisoquinolines by stereoinversion, Green Chem. 21 (20) (2019) 5579–5585, https://doi.org/10.1039/c9gc02795e.
[102] M.M. Musa, I. Karume, M. Takahashi, S.M. Hamdan, N. Ullah, Stereoinversion of *R*-configured secondary alcohols using a single enzymatic approach, ChemistrySelect 3 (36) (2018) 10205–10208, https://doi.org/10.1002/slct.201801673.
[103] R. Feehan, D. Montezano, J.S.G. Slusky, Machine learning for enzyme engineering, selection and design, Protein Eng. Des. Sel. 34 (2021) gzab019, https://doi.org/10.1093/protein/gzab019.
[104] G. Li, Y. Dong, M.T. Reetz, Can machine learning revolutionize directed evolution of selective enzymes? Adv. Synth. Catal. 361 (11) (2019) 2377–2386, https://doi.org/10.1002/adsc.201900149.
[105] Y. Chen, Q. Jiang, L. Sun, Q. Li, L. Zhou, Q. Chen, S. Li, M. Yu, W. Li, Magnetic combined cross-linked enzyme aggregates of ketoreductase and alcohol dehydrogenase: an efficient and stable biocatalyst for asymmetric synthesis of (*R*)-3-quinuclidinol with regeneration of coenzymes in situ, Catalysts 8 (8) (2018) 334, https://doi.org/10.3390/catal8080334.
[106] D. Tokoshima, K. Hanaya, M. Shoji, T. Sugai, Whole-cell yeast-mediated preparation of (*R*)-2-chloro-1-(3-nitrophenyl)ethanol as a synthetic precursor for (*R*)-phenylephrine, J. Mol. Catal. B Enzym. 97 (2013) 95–99, https://doi.org/10.1016/j.molcatb.2013.07.021.
[107] M. Jeong, Y.M. Lee, S.H. Hong, S.Y. Park, I.K. Yoo, M.J. Han, Optimization of enantioselective synthesis of methyl (*R*)-2-chloromandelate by whole cells of *Saccharomyces cerevisiae*, Biotechnol. Lett. 32 (10) (2010) 1529–1531, https://doi.org/10.1007/s10529-010-0396-4.
[108] K. Tsutsumi, T. Katayama, N. Utsumi, K. Murata, N. Arai, N. Kurono, T. Ohkuma, Practical asymmetric hydrogenation of 3-quinuclidinone catalyzed by the XylSkewphos/PICA-ruthenium(II) complex, Org. Process. Res. Dev. 13 (3) (2009) 625–628, https://doi.org/10.1021/op9000302.
[109] F. Dolle, H. Valette, Y. Bramoulle, I. Guenther, C. Fuseau, C. Coulon, C. Lartizien, S. Jegham, P. George, O. Curet, J.L. Pinquier, M. Bottlaender, Synthesis and in vivo imaging properties of [11C] befloxatone: a novel highly potent positron emission tomography ligand for mono-amine oxidase-A, Bioorg. Med. Chem. Lett. 13 (10) (2003) 1771–1775, https://doi.org/10.1016/s0960-894x(03)00215-4.
[110] X. Luo, Y.J. Wang, W. Shen, Y.G. Zheng, Activity improvement of a *Kluyveromyces lactis* aldo-keto reductase *Kl*AKR via rational design, J. Biotechnol. 224 (2016) 20–26, https://doi.org/10.1016/j.jbiotec.2016.03.008.
[111] H. Li, R. Wang, A. Wang, J. Zhang, Y. Yin, X. Pei, P. Zhang, Rapidly and precisely cross-linked enzymes using bio-orthogonal chemistry from cell lysate for the synthesis of (*S*)-1-(2,6-Dichloro-3-fluorophenyl) ethanol, ACS Sustain. Chem. Eng. 8 (16) (2020) 6466–6478, https://doi.org/10.1021/acssuschemeng.0c00987.
[112] J. Kearns, M.M. Kayser, Application of yeast-catalyzed reductions to synthesis of (2r,3s)-phenylisoserine, Tetrahedron Lett. 35 (18) (1994) 2845–2848, https://doi.org/10.1016/S0040-4039(00)76640-8.
[113] R.C. Simon, E. Busto, N. Richter, F. Belaj, W. Kroutil, Chemoenzymatic synthesis of enantiomerically pure syn-configured 1-aryl-3-methylisochroman derivatives, Eur. J. Org. Chem. 1 (2014) 111–121, https://doi.org/10.1002/ejoc.201301429.
[114] X. Chen, Z.Q. Liu, C.P. Lin, Y.G. Zheng, Chemoenzymatic synthesis of (*S*)-duloxetine using carbonyl reductase from *Rhodosporidium toruloides*, Bioorg. Chem. 65 (2016) 82–89, https://doi.org/10.1016/j.bioorg.2016.02.002.